Acad. Sci. USSR, Phys. Ser. 28, 1495 (1964)].
[15]M. G. Davidson, Phys. Letters 22, 596 (1966).
[16]E. Arbman, S. Bjørnholm, and O. B. Nielsen, Nucl. Phys. 21, 406 (1960).
[17]C. M. Lederer, University of California Lawrence Radiation Laboratory Report No. UCRL-11028, 1963 (unpublished).
[18]S. Bjørnholm, F. Boehm, A. B. Knutsen, and O. B. Nielsen, Nucl. Phys. 42, 469 (1963).
[19]S. Bjørnholm, J. Dubois, and B. Elbeck, Nucl. Phys. A118, 241 (1968).
[20]S. Bjørnholm, J. Borgreen, D. Davies, N. J. S. Hansen, and J. Pedersen, Nucl. Phys. A118, 261 (1968).

PHYSICAL REVIEW C VOLUME 2, NUMBER 5 NOVEMBER 1970

Proton Decay of Isobaric Analog Resonances in ^{95}Nb†

Klaus-Peter Lieb
Center for Nuclear Studies, University of Texas, Austin, Texas and Universidad Nacional, Bogota, Colombia

and

James J. Kent,* Till Hausmann,‡ and Charles E. Watson
Center for Nuclear Studies, University of Texas, Austin, Texas 78712
(Received 17 June 1970)

Differential cross sections for elastic and inelastic proton scattering on ^{94}Zr were measured between 6.0- and 8.5-MeV bombarding energy. The decay of analogs of states in ^{95}Zr to the ground state and the 0.92 MeV (2^+), 1.30 MeV (0^+), 1.66 MeV (2^+), and 2.06 MeV (3^-) states in ^{94}Zr was investigated. In the analysis of the inelastic proton groups, the enhancement of the Hauser-Feshbach background, as well as the interference of the resonance amplitude with direct nuclear excitation were taken into account. Spins, spectroscopic factors, and possible weak-coupling configurations in the parent system are derived and compared with results previously obtained for ^{91}Zr and ^{93}Zr.

1. INTRODUCTION

Since the pioneering work of Jones, Lane, and Morrison,[1] inelastic proton scattering through isobaric analog resonances (IAR) has become an efficient tool in nuclear spectroscopy for determining, in a qualitative way, correlations between low-lying core states $|c\rangle$ of the target and the states $|nc\rangle$ of the parent system. Conclusive analyses, however, resulting in numerical values for partial widths and spectroscopic factors, have been performed only for two categories of resonances; namely, single-particle analog resonances (1) built upon the ground state of a target with magic neutron number and decaying to excited neutron-particle–neutron-hole states,[2] and (2) built upon excited core states (weak-coupling model).[3,4]

The partial widths and angular momenta of the outgoing proton partial waves manifest themselves in the shapes of the on-resonance angular distributions. So far, only resonances above a very small background[2] or superimposed on a Hauser-Feshbach background[5-7] have been studied in detail, as those angular distributions feature near symmetry about 90°. However, IAR occur in general at proton energies where Coulomb and direct excitation compete with the resonance process, particularly in exciting collective states. The interference between different modes of excitation can affect an angular distribution to such an extent that details of the resonant part (like the coefficients of the P_4 and higher terms in a Legendre polynomial expansion) are masked. It thus seemed worthwhile to investigate a reaction where the effects of direct scattering have to be taken into account. We chose ^{94}Zr as target and measured the decay of analogs of parent states in ^{95}Zr to target states below 3.0-MeV excitation. From inelastic proton scattering at 12.7 MeV,[8] these states are known to be weakly "deformed," except for the lowest quadrupole and octupole vibrations at 0.92 and 2.06 MeV, respectively, which indeed will show a pronounced nonresonant excitation above 7-MeV proton energy. Because of the very low (p,n) threshold at 1.69 MeV and the high level density in ^{94}Nb, Hauser-Feshbach contributions in the (p,p') cross section from $T_<$ compound states are expected to be small.

The second object of this experiment was to measure spins of IAR and partial widths for the decay to low-lying target states. As was pointed out previously,[5,9] the differential cross section of the protons leaving ^{94}Zr in its excited 0^+ state at 1.30 MeV is most appropriate for this task, since the on-resonance angular distributions depend very sensi-

tively on the spins of the analog states. For resonances observed in both the elastic and inelastic 0^+ channels, this method yields the same information as a polarization measurement[10] of the elastically scattered protons; it surpasses the latter method for those higher parent states whose analogs show up in the excited 0^+ channel as strong and well-separated resonances, where the resonances in the elastic channel are generally very weak and overlap.

The level scheme of ^{95}Zr has been studied by Cohen and Chubinsky[11] via the reactions ^{94}Zr(d,p) and ^{96}Zr(d,t) and by Stautberg *et al.*,[12] who used the reaction ^{96}Zr(p,d). The spin assignments to some states which were populated by $l=2$ and $l=4$ transfers are in disagreement, as Cohen and Chubinsky consider neutron excitation into the $d_{3/2}$ and $g_{7/2}$ orbits, whereas Stautberg *et al.* interpret the same states as neutron hole states in the $d_{5/2}$ and $g_{9/2}$ orbits. Inelastic proton scattering through the analogs of these states and leading to the excited 0^+ state should allow a very sensitive distinction between the two assumptions.

2. EXPERIMENTAL PROCEDURE

2.1. Elastic and Inelastic Proton Scattering

A 510-μg/cm^2-thick zirconium target enriched to 95% in the isotope ^{94}Zr was bombarded with the proton beam of the model EN tandem Van de Graaff of the University of Texas. Elastic and inelastic proton groups were measured in cooled Si(Li) detectors mounted in a conventional 45-cm-diam scattering chamber. The spectra were sampled in a PDP-7 computer, stored on magnetic tape and analyzed on the CDC 6600 computer of the Univer-

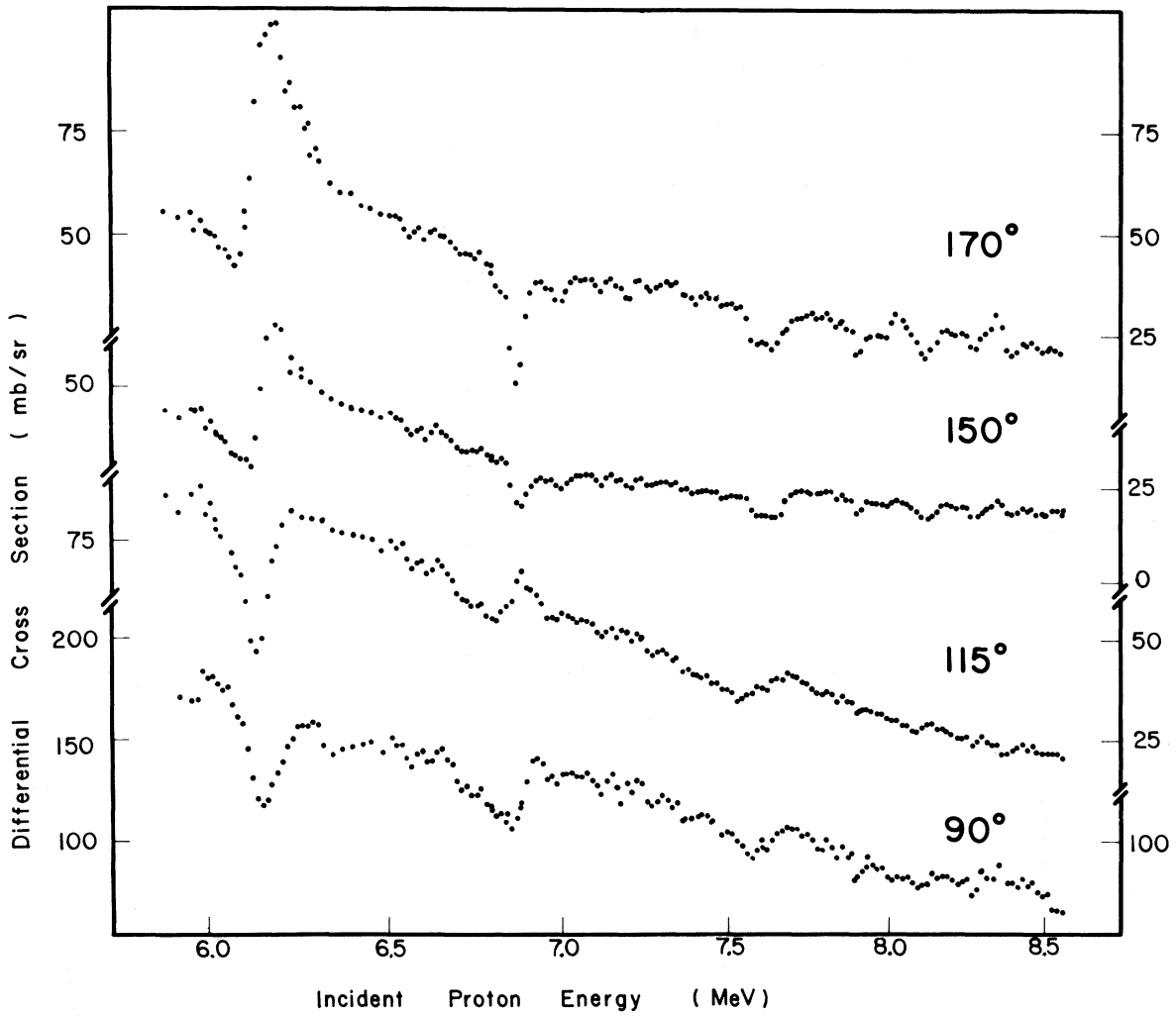

FIG. 1. Excitation functions of elastic proton scattering from ^{94}Zr.

sity of Texas by means of a line-shape fitting program. An integrated beam current of 1000 μC was collected for each data point.

For taking excitation functions at laboratory angles of 90, 115, 150, and 170° with respect to the beam, the proton energy was varied from 6.0 to 8.5 MeV in approximately 17-keV steps. This range covers the analogs of states in ^{95}Zr between 0.95- and 3.30-MeV excitation energy. Figure 1 shows the measured excitation function of the elastic proton group. All resonances except for those at 6.15 MeV ($J^\pi = \frac{1}{2}^+$) and 6.87 MeV ($J^\pi = \frac{3}{2}^+$) are weak in agreement with the small (d,p) spectroscopic factors measured by Cohen and Chubinsky. Excitation functions of inelastic proton groups leaving ^{94}Zr in its excited states at 0.92 (2^+), 1.30 (0^+), 1.66 (2^+), and 2.06 MeV (3^-) are plotted in Fig. 2. The qualitative behavior of inelastic scattering cross sections to different core states appears to be similar to that found for ^{92}Zr as target[13]: The lowest 2^+ state is rather strongly populated at the analogs of nearly all $|nC\rangle$ states up to 2.5-MeV excitation, whereas the 0_2^+ and 2_2^+ channels display a more selective pattern. The excitation function to the 3^- state features three strong resonances between 8.0 and 8.5 MeV. One may note also that the background in the 2_1^+ channel is several times higher than in the other channels. Because of the increasing level density of the parent system above 3.0-MeV excitation energy, the l assignments and spectroscopic factors for those parent states deduced from the (d,p) work are quite uncertain and the respective analog resonances overlap in both the elastic and the 2_1^+ inelastic channel. Therefore, no data were taken above 8.6 MeV, where one does not expect, from analogy to ^{92}Zr, to observe other strong resonances. Figure 3 shows, in more detail, excitation functions to the 0.92-MeV state taken over the 7.58-MeV IAR at several angles. Similarly, Fig. 4 displays excitation functions over the three pronounced resonances

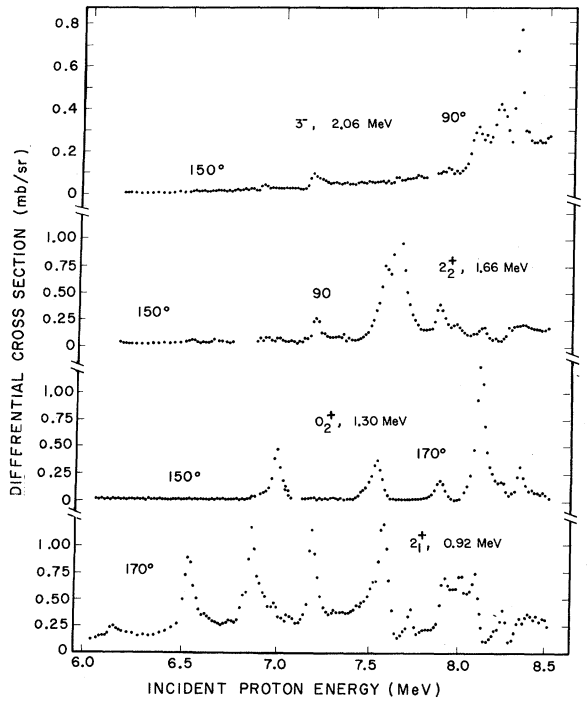

FIG. 2. Excitation functions of inelastic proton groups leaving ^{94}Zr in excited states at 0.92 (2_1^+), 1.30 (0_2^+), 1.66 (2_2^+), and 2.06 MeV (3^-), respectively. The curves were taken at angles at which the respective proton curves were best resolved from contaminants.

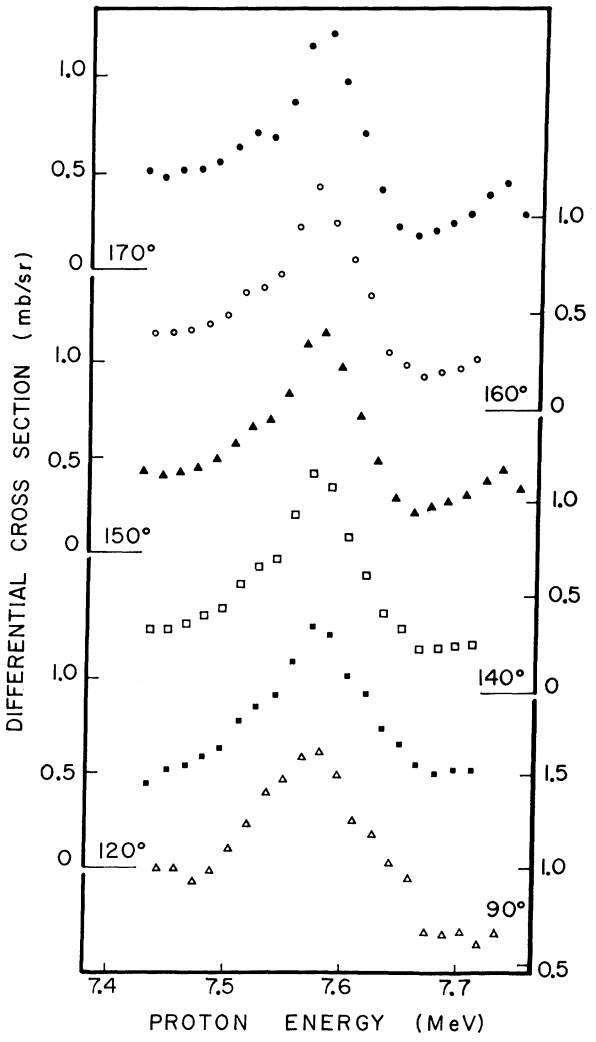

FIG. 3. Excitation functions of the reaction ^{94}Zr(p,p')-0.92 MeV over the 7.58-MeV resonance. Note the decrease of the full width of the peak at backward angles, which indicates interference between direct and resonant excitation of this state.

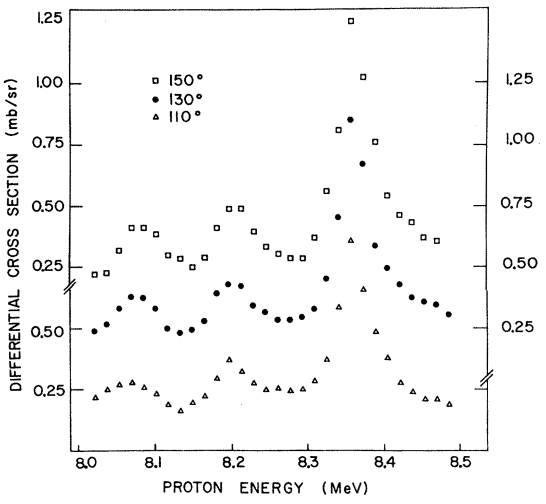

FIG. 4. Detailed excitation functions over the three pronounced resonances in the 2.06 MeV (3^-) channel.

in the 3^- channel.

Angular distributions were measured between 60 and 170° at all prominent resonances and, in particular for the 2_1^+ proton group, at some off-resonance energies. They are plotted in Figs. 5–8 for the inelastic proton groups mentioned above. It is gratifying to see that most of them are symmetric about 90°. Also, for analogs of $|nC\rangle$ states with known spin value J, the highest L values of an expansion in terms of even Legendre polynomials are in agreement with the angular momentum selection rule $L_{\max} \leq 2J-1$. Pronounced deviations from symmetry were found in the angular distributions of protons leading to the 0.92 MeV 2^+ state (Fig. 5) and to the 2.06 MeV 3^- state (Fig. 8). For the resonances in the 3^- channel, a steady increase of the cross section to backward angles was found, a behavior already noted in the $^{92}\mathrm{Zr}(p,p')_{3^-}$ reaction.[13]

Finally, excitation functions and angular distributions of protons to higher excited states at 2.61, 3.05, 3.20, 3.48, and 3.58 MeV were taken over the 8.11-MeV resonance, which appears strongly in the 0_2^+ channel. Figure 9 displays part of the

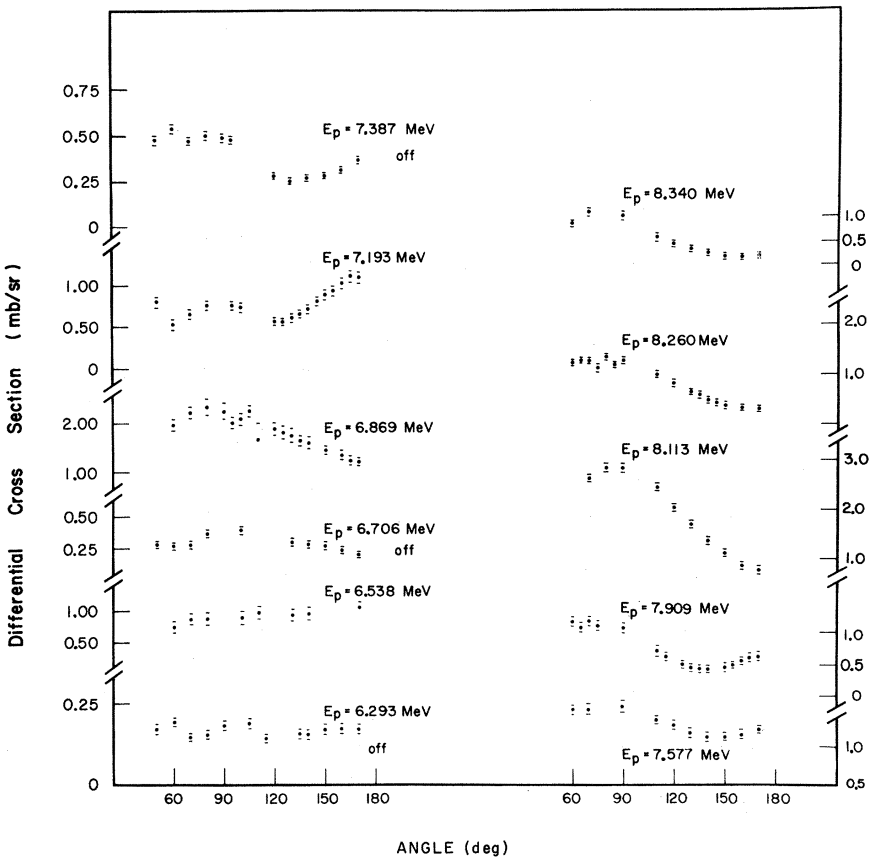

FIG. 5. On- and off-resonance angular distributions for excitation of the 0.92 MeV (2_1^+) state. Effects of direct excitation are visible clearly at 7.387, 7.477, and 7.909 MeV, whereas the off-resonance angular distributions at 6.293 and 6.706 MeV give an estimate of the Hauser-Feshbach contribution.

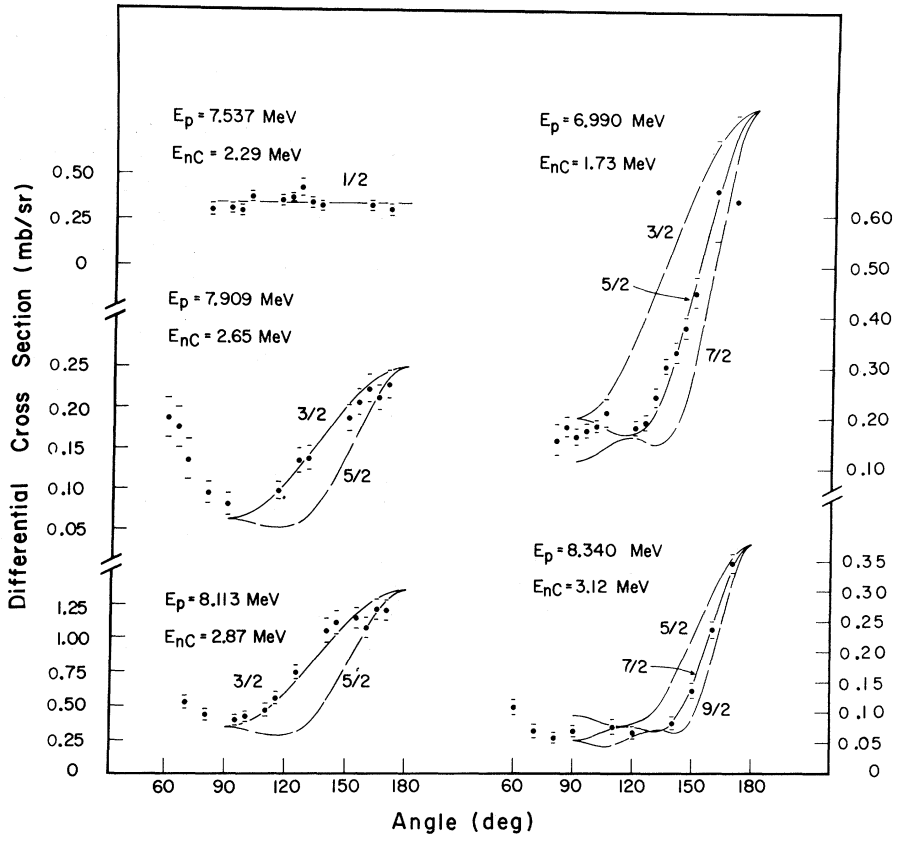

FIG. 6. On-resonance angular distributions of the 1.30 MeV (0_2^+) proton group. Full lines represent the best fits to the experimental points, dashed lines give the predictions for other spin assignments $J' = J \pm 1$. The curves are normalized at 180°. In all cases, the data allow a unique spin assignment.

proton spectrum and a 170° excitation function of these higher proton groups, while Fig. 10 shows their on-resonance angular distributions.

2.2. Determination of Excitation Energies in the Parent Nucleus ^{95}Zr

As mentioned above, the parent nucleus ^{95}Zr has been investigated[11,12] via the reactions ^{94}Zr(d,p), ^{96}Zr(p,d), and ^{96}Zr(d,t). Targets of 5-mg/cm^2 thickness were used in these experiments, and energy resolutions of 75–100 keV for the protons and 120 keV for the deuterons are quoted by the authors. Excitation energies of levels in ^{95}Zr are reported with an uncertainty of 15–25 keV for each reaction but the (p,d) data differ by as much as 200 keV from the (d,p) data. Since the analogs of most parent states do not show up strongly in the ^{94}Zr(p,p_0) excitation function and since the resonances in different inelastic channels are shifted against each other, a more precise determination of excitation energies in the parent system seemed useful in order to be able to unambiguously line up the observed resonances with known $|nc\rangle$ states.

To this end, we briefly studied the reaction ^{94}Zr(d,p). The 510-μg/cm^2 ^{94}Zr target used in the proton work was bombarded with a 7.0-MeV deuteron beam. Protons were detected at 90° to the beam in a Green-type magnetic spectrometer[14] which was equipped with a cooled Si(Li) particle detector placed on the focal surface of the magnet. The magnetic field strength was varied slowly and at a constant rate in order to sweep the different proton groups over the counter. This system works as a particle-identification system, and thus allows one to remove the elastic and inelastic deuteron peaks from the proton spectrum. The energy resolution of 40 keV was limited mostly by the low deuteron energy.

Also, at $E_d = 7.0$ MeV, γ rays from ^{94}Zr$(d,p\gamma)$ were measured in a 56-cm^3 Ge(Li) detector. Due to the high background originating from neutrons and from γ rays following the ^{95}Zr β decay, only the ground-state transitions from the first two excited states in ^{95}Zr at 950 and 1324 keV were ana-

lyzed. In Table I, the results of the (d,p) and $(d,p\gamma)$ runs are compared with previous (d,p) and (d,t) measurements and with the excitation energies deduced from the positions of the IAR. In general, the agreement with the work of Cohen and Chubinsky is very satisfactory. New states in addition to those reported by these authors were localized at 2317 ± 10, 2983 ± 7, and 3061 ± 12 keV.

3. ANALYSIS

3.1. Outline

In general, the purpose of studying inelastic proton scattering at analog resonances is to obtain spectroscopic factors S of the parent system,[15] i.e. the overlap between the configurations of a particular parent state $|nc\rangle$ and that of a single neutron $|n\rangle$ coupled to an excited core state $|c\rangle$: $(S_{clj})^{1/2} \propto \langle nc\,|c \otimes lj\rangle$. This goal is achieved in two steps. From proton excitation functions and angular distributions, the partial widths Γ_{clj} in all measured channels are derived after the effects of nonresonant processes have been taken into account. These experimental partial widths are then compared with model values of single-particle widths Γ^{sp}. It has been pointed out[16] that either $|nc\rangle$ or $|c\rangle$ must have a simple structure in order that the resulting spectroscopic factors can be interpreted and that Γ^{sp} can be calculated. More specifically, if $|nc\rangle$ is known to be a single-neutron state, one can determine the neutron-particle, neutron-hole parts of the wave functions of excited core states; on the other hand, if $|c\rangle$ denotes a pure proton configuration or a highly "collective" state, one selects those parent states which feature a weak-coupling structure.

In the $N = 50$ region, the decay of analogs of low-lying parent states ($E_{nc} \leq 3$ MeV) to the lowest excited target states ($E_c \leq 3$ MeV) has been described exclusively by the weak-coupling approach. This interpretation was based in most cases on the positions, spins, and strengths of the various resonances, but not always proved rigorously by determining the partial waves of the outgoing protons. For the targets ^{88}Sr,[3,17] ^{90}Zr,[4,5] and ^{92}Mo[6,7] with a magic neutron number this procedure may be justified, since neutron excitation across the $N = 50$ gap requires at least 4.5 MeV. However, in the case of ^{94}Zr with four valence neutrons in the $3s2d$ subshell, neutron excitations within this subshell are equally important as proton excitations in the $2p1g$ subshell, making the analysis of angular distributions inevitable. Indeed, spectroscopic factors of two- and single-neutron transfer reactions leading to states in ^{93,94,95}Zr indicate considerable configuration mixing.[11,18,19]

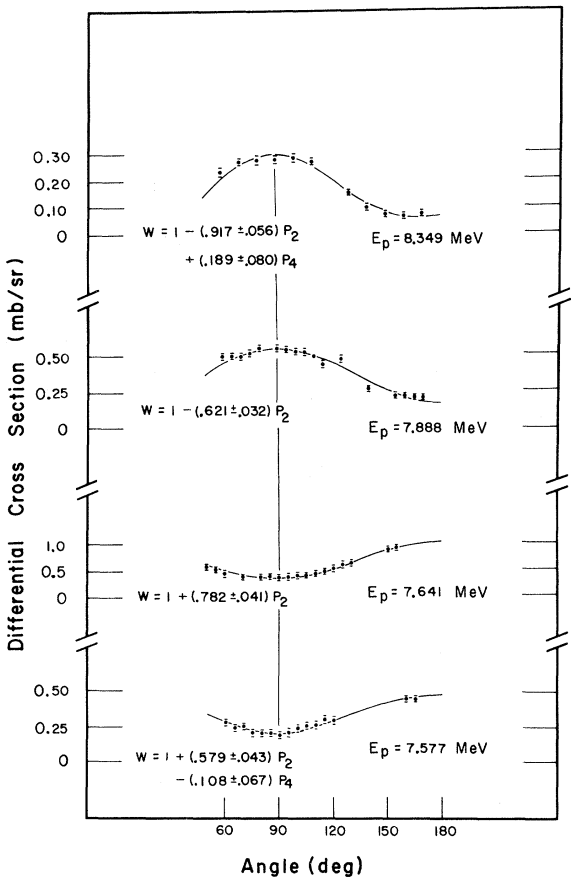

FIG. 7. Angular distributions of the 1.66 MeV (2_2^+) proton group at several resonances. Full lines refer to the Legendre-polynomial expansions $W(\theta) = 1 + \Sigma_k B_k \times P_k(\cos\theta)$ given in the figure.

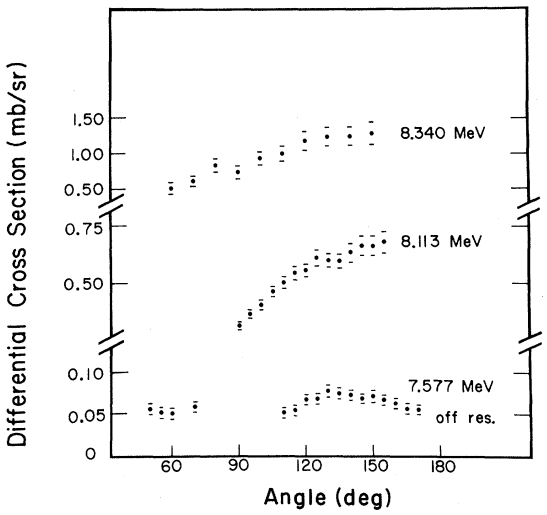

FIG. 8. Angular distributions of the 2.06 MeV (3^-) proton group at the 8.340- and 8.113-MeV resonances, and off-resonance (7.577 MeV).

TABLE I. Excitation energies (in MeV) of parent states in ^{95}Zr. Quoted errors are those of the last digits.

Previous work			Present work		
^{94}Zr(d,p) (Ref. a)	^{96}Zr(d,t) (Ref. a)	^{96}Zr(p,d) (Ref. b)	^{94}Zr(d,p)	^{94}Zr(p,p)	Adopted values
0.95	0.96	1.02(2)	0.950(2)[c]	0.950(8)	0.950(2)
1.33	1.33	1.14(5)	1.324(2)[c]	1.324(4)	1.324(2)
1.64	1.65	...	1.636(5)	1.628(5)	1.632(5)
1.73	1.75	1.79(4)	1.733(10)	1.745(5)	1.739(7)
1.91 [d]	1.92	...	1.913(10)	1.942(5)	1.932(10)
2.03	2.03	2.03(4)	...	...	2.030(25)
2.29	2.30	2.12(5)	...	2.279(10)	2.279(10)
...	...	...	...	2.317(10)	2.317(10)
2.40	2.40	2.37(5)	2.397(15)	2.389(6)	2.391(10)
2.48	...	2.51(4)	...	2.471(10)	2.479(10)
2.65	2.67	...	2.625(20)	2.641(11)	2.636(12)
2.75	2.77	...	2.744(20)	2.744(10)	2.744(12)
2.87	2.88	...	2.847(20)	2.841(12)	2.843(14)
...	...	...	2.985(20)	2.983(5)	2.983(7)
3.03 [d]	3.05	2.97 ?	3.014(20)	3.012(5)	3.012(7)
...	...	...	...	3.061(12)	3.061(12)

[a] From Ref. 11.
[b] From Ref. 12.
[c] From ^{94}Zr($d,p\gamma$).
[d] Possibly several states, Ref. 11.

TABLE II. Spectroscopic factors S_0 for states in ^{95}Zr.

^{94}Zr(d,p) (Ref. a)			^{94}Zr(p,p_0)					
E_{nc} (keV)	lj	S_0	lj (Ref. b)	Γ_0 (keV)	Γ (keV)	Γ_0^{sp} (keV) (Ref. c)	S_0 (Ref. c)	Γ_0^{sp} (keV) (Ref. d)	S_0 (Ref. d)
0	$d_{5/2}$	0.30	...	...	...				
950	$s_{1/2}$	0.89	$s_{1/2}$	40	70	96	0.42	35	1.14
1324	$d_{3/2}$	0.017	$d_{3/2}, d_{5/2}$	~0.8	50	48	~0.017	18.5	~0.043
1632	$d_{3/2}$	0.45	$d_{3/2}$	14	55	54	0.26	21.8	0.64
				10	40		0.18		0.46[e]
				20	50		0.37		0.92[f]
1739	$d_{3/2}$?	0.05	$d_{5/2}$	2.7	42	36.5	0.07	29.0	0.092
1932	$d_{3/2}$	0.078	$d_{5/2}$	2.0	46	60	0.033	27.6	0.073
2030	$g_{7/2}$[g]	0.106	...	...	...				
2279	$p_{3/2}$	0.124	$s_{1/2}$	≤3	66				
2317	...	...	$d_{3/2}$	...	70				
				6	25	71	0.085	34.2	0.175[f]
2391	$d_{3/2}$	0.080		...	57				
2471	$p_{3/2}$	0.024		...	...				
2636	$d_{3/2}$	0.044	$d_{3/2}$	5.0	55	78	0.064	39.9	0.125
2744	$g_{7/2}$	0.26	$g_{7/2}$	2.0	40	4.5	0.45	3.2	0.62
2843	$d_{3/2}$	0.099	$d_{3/2}$	4.0	63	83	0.048	43.8	0.063
2983 3012	$d_{3/2}$	0.093	$d_{3/2}$	3.0	40	88	0.035	48.0	0.063
3061	...	...	$f_{7/2}$	3.0	42	?	?	26.7	0.11

[a] From Ref. 11. Excitation energies from Table I.
[b] From Table IV.
[c] Single-particle widths calculated according to Zaidi and Darmodjo, Ref. 21 and Eq. (5).
[d] Single-particle widths evaluated from the tables of Thompson, Ref. 22.
[e] From Ref. 43.
[f] From Ref. 10.
[g] $h_{11/2}$ in Ref. 53.

The weak-coupling model has the characteristic feature that it predicts a large number of $|nc\rangle$ states with very small (d,p) spectroscopic factors. Consequently, it is often difficult to establish a unique correlation between the observed resonances and the $|nc\rangle$ states identified in the (d,p) reaction, particularly if the parent system has not been explored by complementary experiments, such as inelastic scattering, neutron capture, (p,n) reaction, β decay, etc. The nucleus ^{93}Mo represents an illuminating example for the need of this additional information in order to cover the full weak-coupling multiplets.[6] As mentioned above, the level scheme of ^{95}Zr has been investigated only by single-neutron-transfer reactions. Fortunately, the parent states of all pronounced IAR in inelastic channels, except for three, line up with known states in ^{95}Zr (see Table I).

After these considerations the analysis proceeds in a straightforward way. We first fit the excitation functions of the elastically scattered protons and determine elastic partial widths Γ_0 as well as optical-potential parameters which fit the off-resonance cross section. We then select all resonances in inelastic channels whose angular distributions are symmetric about 90° and attempt to deduce partial waves and partial widths $\Gamma_{c'l'j'}$ for the decay to excited states. Resonances with asymmetric angular distributions are then included in the analysis, and the contributions of the compound inelastic and direct nuclear excitation processes are studied. Finally, we compare the partial widths with single-particle widths and indicate possible weak-coupling configurations of the parent states.

For fitting the differential cross sections and extracting partial widths we are adopting Weidenmüller's theory.[20] Necessary conditions for the applicability of this approach are small nonresonant

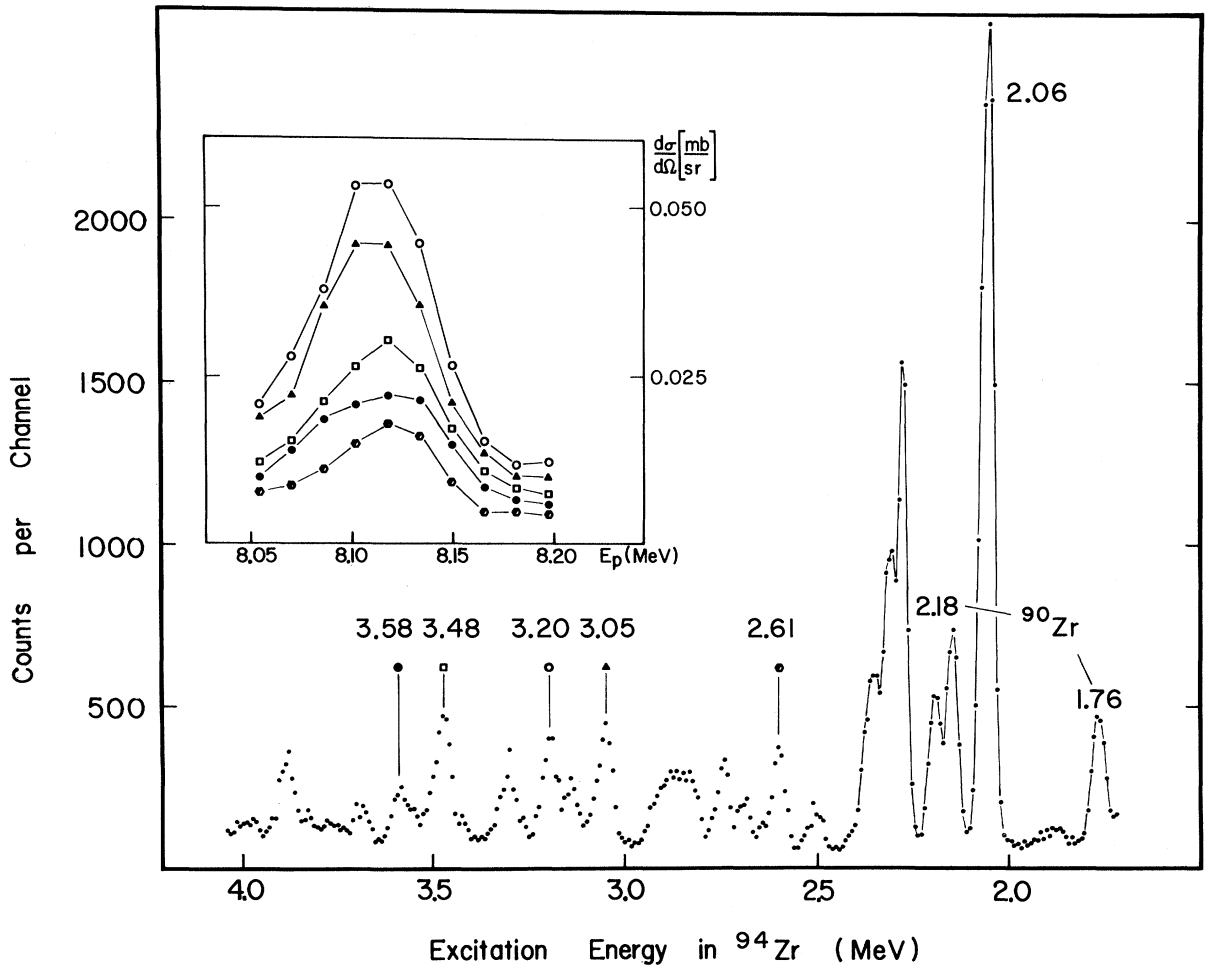

FIG. 9. Part of the proton spectrum of the reaction ^{94}Zr(p,p') taken at 8.11 MeV and $\theta = 120°$. In the insert, 170° excitation functions of proton groups corresponding to higher-lying target states are displayed over the 8.11 MeV ($\frac{3}{2}^+$) resonance.

cross sections and small optical transmission factors as given in the present case. The numerical treatment of inelastic resonance scattering for cases where only a Hauser-Feshbach contribution competes with scattering through IAR and where direct excitation could be negelcted has been discussed thoroughly in earlier papers.[5-7] Hence we shall be mainly concerned here with the influence of direct nuclear excitation. As to the notation we use that of Ref. 6.

3.2. Elastic Scattering Channel

The analysis of (p,p_0) excitation functions over isolated analog resonances in the framework of Weidenmüller's theory, and the derivation of spectroscopic factors is described extensively in earlier works.[21] As usual, the scattering matrix for elastic and inelastic scattering, averaged over the fine structure, is written as

$$\langle S_{cc'}\rangle = S_{cc'}^{\rm opt} + \langle S_{cc'}^{\rm res}\rangle \ . \tag{1}$$

In the resonance part

$$\langle S_{cc'}^{\rm res}\rangle = -i\frac{g_c g_{c'}}{E - E_R + i\Gamma/2}(g^J)^{1/2} \ , \tag{2}$$

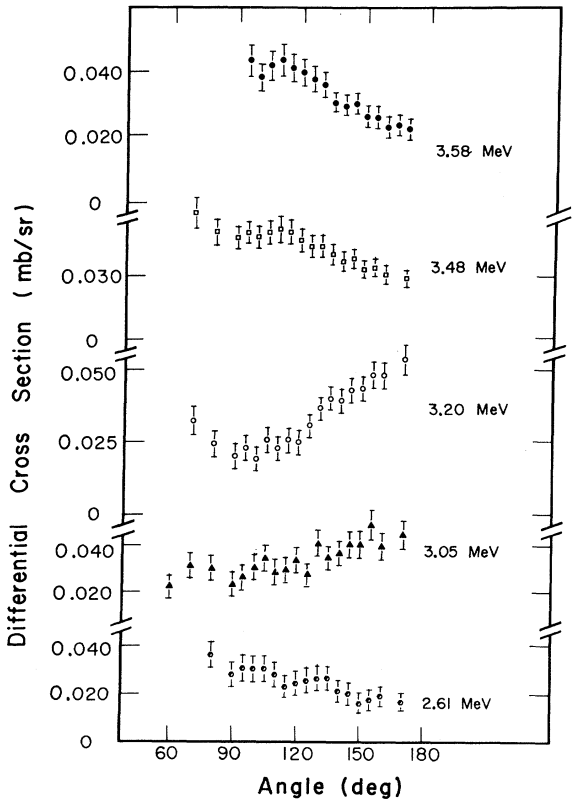

FIG. 10. Angular distributions of the proton groups depicted in Fig. 9, at the 8.11-MeV resonance.

the parameters E_R, Γ, and the complex-valued width functions g_c are modified by the mixing of the analog state with normal $T_<$ states; g^J is the usual statistical factor. Scattering involving these states is simulated by a $|pc\rangle$ optical potential and included in the term $S_{cc'}^{\rm opt}$ in Eq. (1). For analogs in the $N=50$ region, this "feedback" manifests itself in large external spreading widths W_c and, for analogs below the (p,n) threshold, in a considerable enhancement of the Hauser-Feshbach cross section.[6] In addition, each width function is modified by a phase factor $e^{i\phi_c}$, where

$$\phi_c = \xi_c + \rho_c \ , \quad \rho_c \approx 0.5 T_c^{\rm HF}\frac{\Delta_c^{\rm sp}}{\Gamma_c^{\rm sp}} \ , \tag{3}$$

and ξ_c, $T_c^{\rm HF}$, $\Delta_c^{\rm sp}$, and $\Gamma_c^{\rm sp}$ denote the optical-potential phase shift, optical transmission factor, single-particle shift and width, respectively, in channel c. Spectroscopic factors S_{clj} are obtained from the measured partial width Γ_{clj} by applying the relations

$$\Gamma_{clj} = |g_{clj}|^2 = \Gamma_{clj}^A(1-0.5T_{clj}^{\rm HF}) \ , \quad \Gamma_{clj}^A = S_{clj}\Gamma_{clj}^{\rm sp} \ , \tag{4}$$

where Γ_{clj}^A denotes the "natural decay width" in channel c. In most cases the difference between Γ_{clj} and Γ_{clj}^A is negligible.

In searching for an adequate $|pC\rangle$ potential which fits the elastic (and inelastic) off-resonance cross sections, we started with the set D of optical parameters quoted by Dickens, Eichler, and Satchler[8] for scattering on ^{94}Zr at 12.7 MeV. Only slight changes in the real and imaginary well depth $V_p = 59.0 - 0.3E_p$ and $W_D = 8.7$ MeV were necessary to achieve a tolerable fit from 6.0 to 8.5-MeV proton energy. The next step was to analyze the resonance shapes at 90, 115, 150, and 170° by means of the code JULIUS.[21] The quantities E_R and Γ_0 were taken as free parameters and the total width Γ was inserted from the inelastic excitation functions. Spin assignments were taken from the (d,p) work,[11] a polarization measurement,[10] and/or the angular distributions in the inelastic channels (see Sec. 3.3). Resonance parameters corresponding to the best fit are listed in Table II.

In order to deduce spectroscopic factors S_0 in the elastic channel, the single-particle widths were calculated according to the prescriptions of Zaidi[21] and of Thompson.[22] Applying the former method one obtains $\Gamma_{clj}^{\rm sp}$ from the Lane equations[23] by the expression

$$\Gamma_{clj}^{\rm sp} = (k_p/E_p)T_0|\langle na|U_1(r)|pc\rangle|^2 \tag{5}$$

suggested by Stephen.[24] A real volume-type Woods-Saxon potential $U_n(r) + U_1(r)\vec{t}\cdot\vec{T}_0$ was used to evaluate the wave functions $|na\rangle$ and $|pc\rangle$. The well depth $V_n = 49.1$ MeV was adjusted[25] in order to re-

produce the experimental binding energies of the $d_{5/2}$, $s_{1/2}$, and $d_{3/2}$ centers of gravity in ^{95}Zr at 6.23, 5.00, and 4.23 MeV, respectively.[11] The depth of the charge-exchange potential U_1 was fixed to $V_1 = 1.1$ MeV. The radius $R_0 = R_1 = 1.22$ F and diffuseness $a_0 = a_1 = 0.65$ F as well as the spin-orbit potential ($V_{so} = 6.5$ MeV) are the same as for the $|pc\rangle$ potential. This choice of parameters fulfills the two empirical relations

$$V_1 \simeq 104/A \text{ MeV},^{26} \quad V_1 T_0 + V_n \approx V_p .^{27} \tag{6}$$

A second set of single-particle widths was taken from the tables compiled by Thompson.[22] The resulting spectroscopic factors S_0 are compared in Table II with the (d,p) measurement.[11]

The discrepancies between the sets of spectroscopic factors deduced from the (d,p) data and the (p,p_0) IAR data, on the one hand, and between the two sets derived from the IAR data using different definitions of Γ^{sp}, on the other hand, are surprisingly large and even exceed those noted by other authors.[28,29] On the average, it is found that the R-matrix treatment yields spectroscopic factors which are too large by about 35%, whereas the approach of Zaidi and Darmodjo underestimates them by 43%. This trend, but with smaller deviations, was observed already in analog resonance scattering from ^{90,92}Zr and ^{92}Mo targets.[5,6,13,30] It also seems that s- and d-wave resonances feature discrepancies of similar magnitude, as may be seen from the analogs of the 950-keV $\frac{1}{2}^+$ and 1632-keV $\frac{3}{2}^+$ parent states. In view of these shortcomings the extraction of reliable spectroscopic factors in inelastic channels appears most difficult.

3.3. Inelastic Scattering Channels

3.3.1. 1.30 MeV (0_2^+) and 1.66 MeV (2_2^+) States

A quick examination of inelastic scattering excitation functions displayed in Fig. 2 shows that the off-resonance cross sections in the 1.30- and 1.66-MeV channels are very small. Moreover, the on-resonance angular distributions feature symmetry about 90°, and enable us to analyze resonances in these channels by means of the pure Breit-Wigner amplitude $\langle S_{cc'}^{res} \rangle$ defined in Eq. (2).

In the 1.30-MeV channel, five strong resonances were observed which are identified as analogs of states in ^{95}Zr at 1739-, 2279-, 2636-, 2843-, and 3061-keV excitation energy. For each resonance, angular momentum and parity conservation require the partial wave in the exit channel to be the same as that in the entrance channel. This condition produces a characteristic angular distribution from which the spin J of the resonance can be unambiguously determined, as pointed out in Ref. 9. This selectivity is illustrated in Fig. 6, where theoretical angular distributions for different spin values are compared with the measurements. Unique assignments of $J = \frac{5}{2}$, $\frac{1}{2}$, $\frac{3}{2}$, and $\frac{7}{2}$, respectively, could be made to the states mentioned above. The (d,p) work[11] suggests positive parity for the states at 1739, 2636, and 2843 keV; however, (p,p_0) excitation functions over the IAR of the 3061-keV $\frac{7}{2}$ state are consistent with an f-wave resonance, fixing its parity to be negative. As to the 2279-keV $\frac{1}{2}$ state, it was tentatively assigned[11] negative parity and spin $J = \frac{3}{2}$, in disagreement with the isotropic angular distributions of its IAR which infers $J = \frac{1}{2}$. As will be discussed later on, we interpret this state to share a large part of the $[0_2^+ \otimes s_{1/2}]$ weak-coupling strength.

The excitation function of protons exciting the 1.66-MeV (2^+) state feature three pronounced resonances at 7.577-, 7.641-, and 7.888-MeV proton energy (besides several small ones) at which angular distributions were taken (Fig. 7). They correspond to states in ^{95}Zr at 2317-, 2391-, and 2636-keV excitation energy. In general, the decay of an IAR to a target state with nonzero spin can proceed by a mixture of several partial waves. It is well known,[31,32] that one is not able to resolve this mixture from (p,p') angular distributions alone, but needs additional information [from polarization or $(p,p'\gamma)$ correlation measurements[31]] to determine the partial widths. At least this holds as long as no adequate procedures for calculating *ab initio* single-particle widths Γ^{sp} and resonance mixing phases (in inelastic channels as well as elastic) have been developed, thereby reducing drastically the number of unknown parameters. Another difficulty arises from the fact that the two IAR at 7.58 and 7.64 MeV form a doublet as may be seen also in the (p,p_0) excitation functions near 7.6 MeV. Both resonances have been assigned $J^\pi = \frac{3}{2}^+$, the lower one by Wienhard *et al.*[10] from the measured analyzing power of polarized protons, the other from (d,p) angular distributions.[11] However, the result of the polarization experiment seems doubtful, as only one member of the doublet was considered. Apparently, the polarization fit over these resonances, as well as over a similar doublet found in ^{92}Zr(p,p_0) at 7.60 MeV, is not as good as over other isolated resonances (Figs. 7 and 8 of Ref. 10). On-resonance angular distributions of the reaction ^{94}Zr(p,p') to the 1.66-MeV state feature large positive P_2 coefficients at these two IAR. It appears that a two-level R-matrix formalism should be applied, but that differential cross sections taken with a thinner target, in smaller energy steps, and at more angles are required. The IAR at 7.91 MeV, finally, which coincides with the $J^\pi = \frac{3}{2}^+$ resonance in the 1.30-MeV channel, decays to the 1.66-MeV state by the emission of an almost

pure $d_{3/2}$ partial wave, as suggested by the large negative P_2 coefficient $B_2 = -0.62 \pm 0.04$.[33]

3.3.2. 0.92 MeV (2^+) and 2.06 MeV (3^-) States

As mentioned before, the measured differential cross sections of proton groups leading to the 0.92-MeV (2^+) and 2.06-MeV (3^-) states indicate that, in these channels, direct excitation competes with resonance scattering. Evidence comes from the lack of symmetry about 90° of several on- and off-resonance angular distributions above 7.3-MeV proton energy. Even some apparently symmetric distributions have higher terms in their Legendre-polynomial expansions (mostly P_4 terms) than are compatible with the spins of the respective resonances.[33] Furthermore, IAR in the 0.92-MeV channel do not show symmetric Breit-Wigner shapes superimposed on a smoothly varying background as in the 1.30-MeV channel, but rather exhibit long tails and sharp dips (Fig. 2). The off-resonance cross section in the 0.92-MeV channel is considerably higher, having a broad maximum of $\sigma \approx 4.8$ mb near 7.3 MeV. In terms of the scattering matrix given in Eq. (1) the total cross section in the inelastic channel $c' \neq c$ can be written as

$$\sigma_{cc'} = \pi\lambda^2 |S^{\mathrm{dir}}_{cc'} + \langle S^{\mathrm{res}}_{cc'} \rangle|^2 + \sigma^{\mathrm{HF}}_{cc'} , \qquad (7)$$

where $S^{\mathrm{dir}}_{cc'}$ accounts for fast nonresonating processes such as Coulomb and direct-nuclear excitation, and $\sigma^{\mathrm{HF}}_{cc'}$ denotes the contribution from statistical compound-nuclear formation.[20] It seems practical to discuss first the background terms $\sigma^{\mathrm{HF}}_{cc'}$ and $\sigma^{\mathrm{dir}}_{cc'} \propto |S^{\mathrm{dir}}_{cc'}|^2$ off resonance and implement their modification over the resonances afterwards.

The importance of the Hauser-Feshbach term $\sigma^{\mathrm{HF}}_{cc'}$ at resonances occurring below the (p,n) threshold was emphasized in several recent analyses.[5-7,34] At resonances in ^{91}Nb and ^{93}Tc, for instance, it was noted that the enhancement of $\sigma^{\mathrm{HF}}_{cc'}$ due to mixing of the IAR with $T_<$ states can amount to as much as 75% of the observed peak and that this enhanced contribution has to be subtracted before reliable spectroscopic factors can be derived. In the present case, however, the ^{94}Zr(p,n) threshold lies at $E_p = 1.69$ MeV, so that in the range of proton energies studied here the $T_<$ compound states feed mainly neutron channels leading to the many levels of the odd-odd nucleus ^{94}Nb (Ref. 35). It is consistent with this remark that the measured off-resonance (p,p') cross section in the 0.92-MeV channel ($\sigma = 2-5$ mb) is smaller by an order of magnitude than in the reaction ^{92}Mo(p,p') to the 1.52-MeV 2^+ state where IAR lie several MeV below the (p,n) threshold.[6] In the other inelastic channels of ^{94}Zr(p,p'), Hauser-Feshbach contributions are negligible (Fig. 2).

Unfortunately, the large number of states in ^{94}Nb with unknown spins and parities do not allow an exact evaluation of $\sigma^{\mathrm{HF}}_{cc'}$ in the case of ^{94}Zr(p,p'). Nevertheless, we attempted to estimate this quantity in the vicinity of the 6.87 MeV $\frac{3}{2}^+$ resonance in order to set an upper limit on the enhanced contribution. In the presence of many open neutron channels, this enhanced part is given by

$$\sigma^{\mathrm{HF,enh}}_{cc'} = \pi\lambda^2 g^J T_p T_{p'} \Big(\sum_n T^{\mathrm{HF}}_n + T_p + T_{p'}\Big)^{-1} , \qquad (8)$$

where T_p and $T_{p'}$ denote modified proton transmission factors

$$T = T^{\mathrm{HF}} \frac{(E - E_R + \Delta)^2 + \omega^2}{(E - E_R)^2 + \Gamma^2/4} . \qquad (9)$$

For the test calculation, the parameters $E_R = 6869$ keV, $\Gamma = 45$ keV, $\Delta = -60$ keV, and $\omega \simeq 10$ keV were chosen[6] in the elastic and 0.92-MeV channel. The transmission coefficients were computed from the $|pc\rangle$ optical potential mentioned in Sec. 3.2. As for the denominator of Eq. (8), we used Beyster's neutron transmission factors for $(^{90}\mathrm{Zr} + n)$ [36] and considered the 83 final states in ^{94}Nb below 2.7-MeV

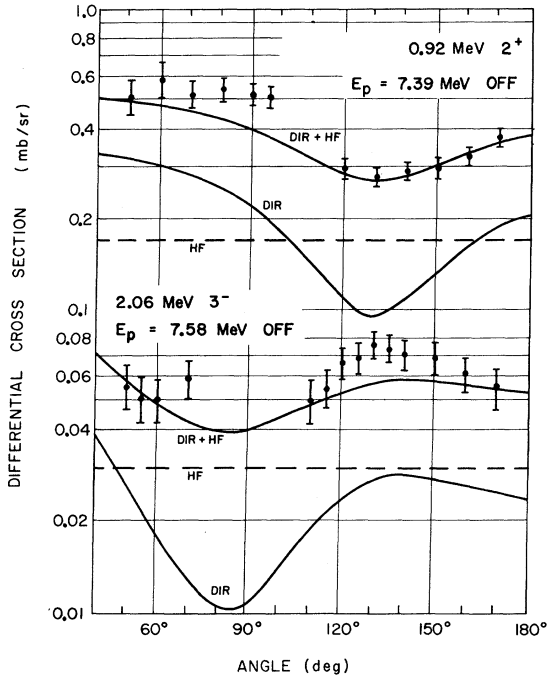

FIG. 11. Off-resonance angular-distributions in the 0.92-MeV (2^+) channel (at 7.39 MeV) and the 2.06-MeV (3^-) channel (at 7.58 MeV). The fits to the data, labeled DIR+HF, are obtained by adding a Hauser-Feshbach estimate HF to the DWBA cross section, DIR, calculated with the program JUPITER. The coupling parameters reported, $\beta_2 = 0.13$ and $\beta_3 = 0.18$, and the optical parameters reported in Ref. 8 (except $V_0 = 56.8$ MeV, $W_D = 8.7$ MeV) were used.

excitation energy quoted in Ref. 35. Lacking other information, spins and parities of levels in ^{94}Nb with unknown J^π were assumed to be randomly distributed with $J^\pi \leq 7^\pm$. This estimate yields $\sigma_{cc'}^{HF}$ = 2.6 mb at the resonance and $\sigma_{cc'}^{HF}$ = 2.0 mb off resonance, i.e., an enhancement of 0.6 mb or 3% of the observed peak cross section of 18 mb. These numbers represent upper limits, since the open neutron channels above 2.7-MeV excitation were not considered. The calculation was repeated with only the 15 lowest states in ^{94}Nb included, and the same ratio between on- and off-resonance Hauser-Feshbach cross sections was obtained. In conclusion, we note (what intuitively is obvious) that for strong analog resonances occurring several MeV above the (p,n) threshold, the enhancement of the Hauser-Feshbach background is negligible, even if the nonenhanced part has to be accounted for, and that the observed deviations from Breit-Wigner shapes are due to effects of direct excitation.

Off-resonance effects of direct excitation were observed in the angular distributions taken at 7.39 MeV in the 2^+ channel, and at 7.58 MeV in the 3^- channel (Fig. 11). No off-resonance data were measured for higher energies, since the tails of the resonances overlap (Fig. 2). We calculated $(d\sigma/d\Omega)^{dir}$ at 7.39 and 7.58 MeV using Tamura's coupled-channel code JUPITER[37] in its simplest two-channel distorted-wave Born approximation (DWBA) version, i.e., with one excited state (either 2^+ or 3^- phonon state) coupled to the ground state. As coupling constants we chose the collective parameters β_2 = 0.13 and β_3 = 0.18 derived from ^{94}Zr(p,p') experiments at 12.7[8] and 19.4 MeV.[38] These theoretical angular distributions (labeled DIR) are displayed in Fig. 11. They reproduce the general shape of the measured distributions, but underestimate them by a factor of about 2. The missing cross section may be interpreted as the Hauser-Feshbach contribution[39] and can be extrapolated, in the 2^+ channel, from the off-resonance angular distributions at 6.29 and 6.71 MeV (Fig. 5) which are symmetric about 90°. At 7.39 MeV, we thus added the isotropic cross section $(d\sigma/d\Omega)^{HF}$ = 0.17 mb/sr measured at 6.29 MeV.[40] At 7.58 MeV, an *ad hoc* estimate of $(d\sigma/d\Omega)^{HF}$ = 0.03 mb/sr for all angles had to be added in order to fit the data. The resulting curves labeled DIR+HF in Fig. 11 still underestimate the experimental points by about 15% at the peaks. It is worthwhile to note that no optical parameters were readjusted, but that the same set was used as for fitting the background in the elastic channel. Coulomb excitation was not taken into account.

The last step of the analysis was the evaluation of the interference between resonance and direct scattering. To this end, the program JUPITER was modified, according to Eq. (7), in order to allow for resonances in all inelastic channels to be coupled together. (This feature, though not applied in the present two-channel version, might be advantageous to use in cases where a more complicated coupling scheme is desirable, for instance, if the core states are part of a rotational band or a phonon spectrum.) As pointed out by Tamura, the DWBA cross section, $(d\sigma/d\Omega)_{cc'}^{dir}$, is calculated in JUPITER from the "C matrix" [see Eq. (47) of Ref. 37, and Ref. 41]. Because of the decomposition of the C matrix into partial waves, each matrix element $C_{0lj;c'l'j'}^{J,dir}$ refers to the total angular momentum $J=j$ in the case of a 0^+ target, and an outgoing partial wave $l'j'$ in channel c'. If the resonance scattering proceeds through a combination of angular momenta $(lj;l'j')$, for instance, we added a resonance term [see Eq. (2)] to the respective matrix elements $C_{0lj;c'l'j'}^{J,dir}$. The program then calculates the proper angular distribution without further changes. As a test, we set the coupling parameters β_2 or β_3 equal to zero and compared the resulting angular distributions with those calculated from standard references.[42,33]

In Fig. 12, the effect of the interference is illustrated for the particular choice of $d_{3/2}$ waves in the elastic and 0.92-MeV 2^+ channels, for the parameters E_R = 8113 keV, Γ = 63 keV, and $\Gamma_0 = \Gamma_{1d_{3/2}}$ = 10 keV. The relative phase between resonant and DWBA excitation was set to zero; resonance mixing phases, ρ_c, the Hauser-Feshbach background, and Coulomb excitation were neglected. It is gratifying to see that between 60 and 140° the curve labeled RES+DIR deviates very little from the pure-resonance angular distribution RES. Effects of direct excitation are visible at forward and backward angles; the 170° excitation function, for instance, shows a pronounced interference pattern, in contrast to the Breit-Wigner shape predicted at 130°. It is interesting to note that the theoretical "total width" [= full width at half-maximum (FWHM)] of the resonance peak decreases toward backward angles. This behavior was observed for the 7.58-MeV resonance (Fig. 3). Also inserted in Fig. 12 are the measured cross sections at the 8.11-MeV $\frac{3}{2}^+$ resonance which verify the assumed $d_{3/2}$ partial wave in the 2_1^+ channel.

A strong negative P_2 term was also found in the angular distribution of the 8260-keV $\frac{3}{2}^+$(?) resonance which suggest a $d_{3/2}$ partial wave in the decay to the 2_1^+ channel. Angular distributions at the $\frac{3}{2}^+$ IAR at 7909 and 7577 keV are very similar in shape to the off-resonance distribution at 7387 keV (Figs. 6 and 11); subtracting the latter from the former, therefore, leaves nearly isotropic resonance distributions. Further discrimination between s wave (B_2 = 0), $d_{5/2}$ wave (B_2 = −0.114), or a

mixture of partial waves was uncertain; however, for the 7577-keV resonance, the large partial width was taken to indicate a predominant $s_{1/2}$ contribution. The same objection holds for the $\frac{3}{2}^+$ IAR at 6869 keV having $B_2 = -0.36 \pm 0.05$. The nearly isotropic 6538-keV resonance is thought to decay predominantly by s-wave emission; its parent state at 1324 keV will be interpreted to have principally a $[2_1^+ \otimes s_{1/2}]$ weak-coupling configuration. Unfortunately, the present data give no hint on the spin of this state which variously has been assumed to be $J = \frac{5}{2}$ (Refs. 12, 43) or $J = \frac{3}{2}$ (Ref. 11). The P_4 term in the angular distribution at 7193 keV, finally, is partly due to direct excitation, but reveals also a P_4 term in the resonance term from which we made the tentative spin assignment $J = \frac{5}{2}$.

Having estimated the off-resonance cross sections $\sigma_{cc'}^{\mathrm{HF}} + \sigma_{cc'}^{\mathrm{dir}}$ and having found the on-resonance interference term between direct and resonant excitation quite small (at least for the particular case mentioned above), the evaluation of resonance cross sections $\sigma_{cc'}^{\mathrm{res}}$ and partial widths $\Gamma_{c'}$ in inelastic channels

$$\Gamma_{c'} = \sum_{l'j'} \Gamma_{c'l'j'} = \sigma_{cc'}^{\mathrm{res}} \frac{\Gamma^2}{\Gamma_0} \frac{1}{2\pi\lambda^2(2J+1)} \tag{10}$$

is straightforward. All resonance parameters for the decays into inelastic channels are summarized in Table III and are discussed in the next section. It should be pointed out that for resonances where $\Gamma_0 \lesssim 3$ keV the uncertainty in extracting Γ_0 is large (perhaps 50%). Consequently, the $\Gamma_{c'}$ and spectroscopic factors will reflect this uncertainty in these cases.

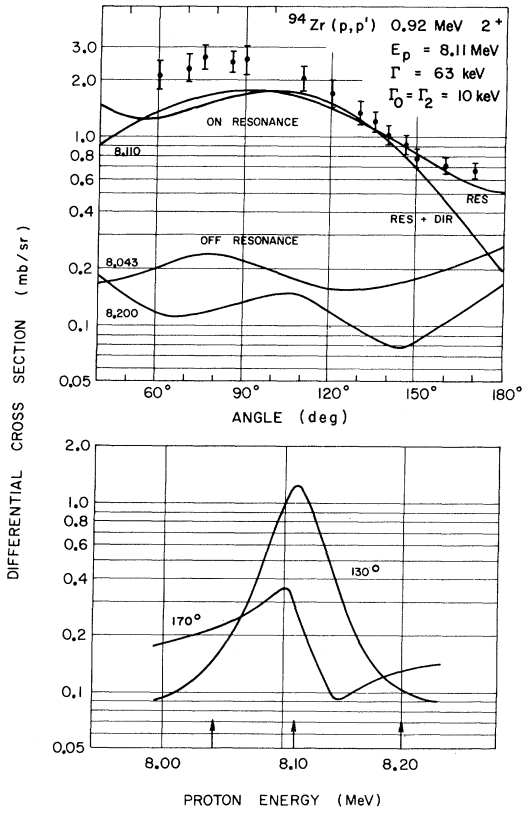

FIG. 12. Theoretical angular distributions and excitation functions over the $\frac{3}{2}^+$ resonance at 8.11 MeV, assuming interference between the resonant and DWBA amplitudes (RES+DIR). A spin sequence $0^+(d_{3/2})\frac{3}{2}^+(d_{3/2})2^+$, and widths $\Gamma = 63$ keV, $\Gamma_0 = \Gamma_{1d\,3/2} = 10$ keV were assumed in the test calculation. The curve labeled RES refers to a pure resonance mechanism. Experimental points are taken from Fig. 5.

4. RESULTS AND DISCUSSION

4.1. Resonance Parameters and Spin Assignments

Results of the present experiment are summarized in Tables II–V. Table II lists the total widths Γ, the partial widths in the elastic channel Γ_0, and two sets of spectroscopic factors S_0 derived from them. A critical discussion of these numbers was already given in Sec. 3.2.

Resonance parameters which specify the decays of IAR to excited target states are presented in Table III. Large partial widths in inelastic channels were observed at 6538 (2_1^+), 7537 (0_2^+), 7577 (2_1^+), 7909 (2_2^+), 8113 ($0_2^+, 2_1^+$), and 8340 keV (3^-). At each of these resonances the predominant partial wave $l'j'$ of the outgoing protons could be identified as $s_{1/2}$ or $d_{3/2}$. For the other resonances in the 2_1^+ and 2_2^+ channels, we obtained smaller widths $\Gamma_{c'}$, and were not able to extract a dominant decay partial wave. Clearly, even large $d_{5/2}$ and $g_{7/2}$ contributions were not detectable, because of the small single-particle widths and/or small angular-distribution coefficients B_2 of these partial waves.

The very small resonance in the 2_1^+ channel observed at 6112 keV (analog of the 950-keV $\frac{1}{2}^+$ parent state) deserves special attention. Two mechanisms are likely to produce this peak. It can be due to a mixing of the $[0_1^+ \otimes s_{1/2}]$ and $[2_1^+ \otimes d_{5/2}]$ weak-coupling configurations whose zeroth-order energies are degenerate at about 0.92 MeV. The inelastic protons are emitted as $d_{5/2}$ partial wave with decay width $\Gamma_{1d\,5/2} = 0.5$ keV. Since the channel energy coincides with the resonance energy $E_R = 5.21$ MeV of the ^{95}Zr ground-state analog, the single-particle width $\Gamma_{1d\,5/2}^{\mathrm{sp}}$ can be evaluated from the partial width $\Gamma_0 = 2.0$ keV (Refs. 10, 44) and spectroscopic factor $S_0 = 0.30$ (Ref. 11) of the latter resonance: $\Gamma_{1d\,5/2}^{\mathrm{sp}} = 2.0/0.30 = 6.7$ keV. One thus obtains $S_{1d\,5/2} = 0.075$ for the $[2_1^+ \otimes d_{5/2}]$ admixture of the 950-keV state, and a normalization of $S_{0s\,1/2} + S_{1d\,5/2} = 0.975$. If, on the other hand, the wave function of the 0.92-MeV 2_1^+ core state contains a "particle-

hole" component of the type $[\nu(s_{1/2})\nu^{-1}(d_{5/2})]|0\rangle$, this admixture would be populated by the $|nA\rangle$ part of the IAR,

$$\{\nu(s_{1/2})[\pi(d_{5/2})\nu^{-1}(d_{5/2})]_0\}_{1/2}|0\rangle \ . \qquad (11)$$

Here, $|0\rangle$ denotes the ^{94}Zr ground state to be taken as $|0\rangle = \nu^4(d_{5/2})$. One can estimate $|C_{\rm ph}|^2$, the spectroscopic factor for the particle-hole component $[\nu(s_{1/2})\nu^{-1}(d_{5/2})]|0\rangle$ in the 2_1^+ state, from the partial width $\Gamma_{1d_{5/2}} = 0.5$ keV to be

$$|C_{\rm ph}|^2 \leq \frac{3\Gamma_{1d_{5/2}}}{5\Gamma^{\rm sp}_{1d_{5/2}} S_{0s_{1/2}}} = 5\% ,$$

where the factor $\frac{3}{5}$ arises from recoupling[3] the angular momenta in expression (11) and the fact that one of four $d_{5/2}$ neutrons can be excited.

The presence of a $[\nu(s_{1/2})\nu^{-1}(d_{5/2})]|0\rangle$ contribution was already suggested by Beery[18] in the analysis of ^{92}Zr(t,p) data. He pointed out that the 0.92-MeV state in ^{94}Zr is excited three times as strongly as predicted from a pure $[\nu^4(d_{5/2})]_2$ shell-model configuration, but that the spectroscopic factor of the ^{90}Zr(t,p) reaction to the 2_1^+ state in ^{92}Zr favors a pure $[\nu^2(d_{5/2})]_2$ configuration of the latter state. Shell-model calculations[19] and recent lifetime measurements[45,46] of the 2_1^+ and 0_2^+ states in ^{92}Zr and ^{94}Zr point to a higher degree of mixing among the $(3s2d)$ neutron orbits in ^{94}Zr than in ^{92}Zr. On the other hand, there exist two arguments in favor of the weak-coupling explanation. First, a peak of similar strength was observed in the reaction ^{92}Zr$(p,p')2_1^+$ at the resonance of the corresponding $s_{1/2}$ single-neutron state in ^{93}Zr. If interpreted in terms

TABLE III. Resonance parameters for the decay of the IAR in ^{95}Nb to excited target states.

E_{nc} (keV)	E_R (keV)	J^π	$l'j'$ (Ref. a)	B_2 (Ref. b)	B_4 (Ref. b)	B_6 (Ref. b)	$\sigma^{\rm res}$ (Ref. c) (mb)	Γ (keV)	$\Gamma_{c'}$ (Ref. d) (keV)
1.30-MeV 0^+ state									
1739	6990	$\frac{5}{2}^{(+)}$	$d_{5/2}$	$+1.14\pm0.08$	$+0.86\pm0.10$		3.4	42	2.0
2279	7537	$\frac{1}{2}^{(+)}$	$s_{1/2}$				4.3	66	$\geq 18.$
2636	7909	$\frac{3}{2}^+$	$d_{3/2}$	$+0.80\pm0.06$			1.6	55	1.5
2843	8113	$\frac{3}{2}^+$	$d_{3/2}$	$+0.82\pm0.06$			8.6	63	13.3
3061	8340	$\frac{7}{2}^-$	$f_{7/2}$	$+1.08\pm0.10$	$+1.03\pm0.15$	$+0.82\pm0.15$	1.2	42	0.6
1.66-MeV 2^+ state									
2317	7577	$(\frac{3}{2}^+)$		$+0.58\pm0.06$	-0.11 ± 0.09		4.8	70	
2391	7641	$(\frac{3}{2}^+)$		$+0.78\pm0.06$			8.5	(57)	
2636	7888	$\frac{3}{2}^+$	$d_{3/2}$	-0.62 ± 0.04			7.8	55	7.2
0.92-MeV 2^+ state									
950	6112	$\frac{1}{2}^+$					1.5	75	0.5
1324	6538	$(\frac{5}{2}^+)$	$s_{1/2}$	$+0.12\pm0.08$ [e]			8.1	50	$\sim 22.$
1632	6869	$\frac{3}{2}^+$		-0.36 ± 0.05 [e]			18.2	55	5.2
1932	7193	$(\frac{5}{2}^+)$	$s_{1/2}$	$+0.26\pm0.06$ [e]	$+0.38\pm0.07$		7.0	46	6.8
2317	7577	$\frac{3}{2}^+$	$s_{1/2}$	-0.16 ± 0.07 [e]			12.8	70	15.2
2636	7909	$\frac{3}{2}^+$					?	55	?
2843	8113	$\frac{3}{2}^+$	$d_{3/2}$	-0.70 ± 0.15 [e]			8.3	63	12.8
2983	8260	$(\frac{3}{2}^+)$	$d_{3/2}$	-0.84 ± 0.15 [e]			6.8	?	?

[a] Predominant partial wave in inelastic channel.
[b] Resonant angular distribution $W(\theta) = 1 + B_2 P_2 + B_6 P_6$.
[c] Estimated resonance cross section (for details see text).
[d] Sum of partial widths in inelastic channel $\Gamma_{c'} = \sum_{lj} \Gamma_{c'l'j'}$.
[e] Corrected for background.

of the particle-hole concept, this peak would contradict Beery's results.[18] Furthermore, Legg, Crosby, and Roy[43] reported on a ^{94}Zr$(p,p')2_1^+$ experiment in which they detected a peak even at the lowest $\frac{5}{2}^+$ resonance at 5.21 MeV. They found the on-resonance angular distribution to have a significant P_4 term. However, their angular distribution includes mainly forward angles. The forward peaking they observe may very well result from the direct contribution to the cross section for the 2_1^+ state. (This same argument would tend to negate their assignment of $J=\frac{5}{2}$ to the resonance they observe at 6.86 MeV, the analog of the 1632-keV level in ^{95}Zr.) Therefore, no definite conclusion on this point can be reached at the present time.

The spins of five states in ^{95}Zr were determined from angular distributions in the 1.30-MeV 0_2^+ channel, and that of at least four more states assigned with high probability from angular distributions in the 2_1^+ channel. Table IV compares these values with previous assignments.[10-12,43] Two $\frac{1}{2}^+$ states and several $\frac{3}{2}^+$ states are expected from similarity to ^{93}Zr[13] and ^{91}Zr.[15] The occurrence of three or four $\frac{5}{2}^+$ states is somewhat surprising, since the ^{95}Zr ground state is known to exhaust 90% of the full shell-model strength $S_0=0.33$,[11] and since only two (one) $\frac{5}{2}^+$ states were identified in ^{91}Zr (^{93}Zr).[5,11,13] Vervier[19] predicts $\frac{5}{2}^+$ states at 0-, 1706-, 2182-, and 2975-keV excitation energy, but only the ground state should show up in the ^{94}Zr-(d,p) reaction. The $\frac{5}{2}^+$ assignments to the states at 2391, 2471, and 2983 keV made in a ^{96}Zr(p,d) experiment[12] have not been established in our analysis. However, it is not unlikely that the states seen in the ^{96}Zr(p,d) experiment are not the same as those studied by us. Indeed, Vervier's calculations[19] and the large number of states in ^{93,95}Mo and ^{94}Nb with very small (d,p) spectroscopic factors reported by Moorhead and Moyer[35] favor this explanation.

4.2. Weak-Coupling States in ^{91,93,95}Zr

States in ^{91,93,95}Zr whose analogs were found to decay predominantly by *one* partial wave lj to *one* core state c, with a large partial width Γ_{clj}, are

TABLE IV. Spins and parities of states in ^{95}Zr. Spin-parity assignments listed in columns two and three are based on the l values determined in single-neutron transfer reactions (Refs. 11 and 12). The first spin value in each column gives the choice of the authors of Refs. 11 and 12, respectively; the second number is the other spin value compatible with l.

State E_{nc} (keV)	Previous work (Ref. a)	Previous work (Ref. b)	Previous work (Ref. c)	Previous work (Ref. d)	Present work	Adopted
0	$\frac{5}{2}^+$	$\frac{5}{2}^+$	$\frac{5}{2}^+$	$\frac{5}{2}^+$		$\frac{5}{2}^+$
950	$\frac{1}{2}^+$	$\frac{1}{2}^+$		$(\frac{1}{2}^+)$	$\frac{1}{2}^+$	$\frac{1}{2}^+$
1324	$\frac{3}{2}^+, \frac{5}{2}^+$	$\frac{5}{2}^+, \frac{3}{2}^+$		$(\frac{5}{2}^+)$		
1632	$\frac{3}{2}^+$		$\frac{3}{2}^+$	$\frac{5}{2}^+$	$(\frac{3}{2}^+)$	$\frac{3}{2}^+$
1739	$(\frac{3}{2}^+)$				$\frac{5}{2}^{(+)}$	$\frac{5}{2}^+$
1932	$\frac{3}{2}^+, \frac{5}{2}^+$				$(\frac{5}{2}^+)$	$(\frac{5}{2}^+)$
2030	$\frac{7}{2}^+, \frac{9}{2}^+$	$\frac{9}{2}^+, \frac{7}{2}^+$				$\frac{11}{2}^-$ [e]
2279	$(\frac{3}{2}^-)$				$\frac{1}{2}^{(+)}$	$\frac{1}{2}^+$
2317			$(\frac{3}{2}^+)$		$(\frac{3}{2}^+)$	$(\frac{3}{2}^+)$
2391	$\frac{3}{2}^+, \frac{5}{2}^+$	$\frac{5}{2}^+, \frac{3}{2}^+$			$(\frac{3}{2}^+)$	$(\frac{3}{2}^+)$
2471	$(\frac{3}{2}^-)$	$\frac{5}{2}^+, \frac{3}{2}^+$				
2636	$(\frac{3}{2}^+)$				$\frac{3}{2}^+$	$\frac{3}{2}^+$
2744	$\frac{7}{2}^+, \frac{9}{2}^+$				$(\frac{7}{2}^+)$	$(\frac{7}{2}^+)$
2843	$\frac{3}{2}^+, \frac{5}{2}^+$				$\frac{3}{2}^+$	$\frac{3}{2}^+$
2983						
3012	$\frac{3}{2}^+, \frac{5}{2}^+$	$\frac{5}{2}^+, \frac{3}{2}^+$			$(\frac{3}{2}^+)$	$(\frac{3}{2}^+)$
3061					$\frac{7}{2}^-$	$\frac{7}{2}^-$

[a] See Ref. 11.
[b] See Ref. 12.
[c] See Ref. 10.
[d] See Ref. 43.
[e] See Ref. 53.

listed in Table V. Based on their energies and/or spins, the three $[0_2^+ \otimes lj]$ states in ^{91}Zr were interpreted by Moore and collaborators[4] as weak-coupling states. Detailed analog studies on ^{90,92,94}Zr targets[5,13] have revealed the existence of at least 14 more states of this nature and have confirmed that indeed the partial wave predicted by the model is emitted in the inelastic channel. We have also demonstrated that, for core states with $J_c \neq 0$, inelastic proton scattering allows only the unambiguous identification of $s_{1/2}$ and $d_{3/2}$ weak-coupling states. Those with the single neutron in a $d_{5/2}$ or $g_{7/2}$ orbit may be studied by means of polarization[47] or $(p,p'\gamma)$ correlation techniques.[31] In some cases, the measurement of γ-ray angular distributions helps to determine the components with small decay widths.[5]

Turning back to Table V, we note that the 0_2^+ lev-

TABLE V. Possible weak-coupling states in ^{91,93,95}Zr.

Core state c	Partial wave lj	A	E_{nC} (MeV)	E_{clj} (MeV)	J^π	S_0 (Ref. a)	Γ_{clj} (keV)	S_{clj}	Reference
0_1^+	$d_{5/2}$	91	0	0	$\frac{5}{2}^+$	0.89	4.0		34
		93	0	0	$\frac{5}{2}^+$	0.54	4.0		10,44,50
		95	0	0	$\frac{5}{2}^+$	0.30	2.0		10,44
	$s_{1/2}$	91	1.21	0	$\frac{1}{2}^+$	0.72	38		30,44
		93	0.96	0	$\frac{1}{2}^+$	0.91	38		13,30,44,51
		95	0.95	0	$\frac{1}{2}^+$	0.89	41		44
	$d_{3/2}$	91	2.06	0	$\frac{3}{2}^+$	0.45	15		5,10,30,44
		93	1.45	0	$\frac{3}{2}^+$	0.38	13		10,13,44,50
		95	1.63	0	$\frac{3}{2}^+$	0.45	15		10,43,44
0_2^+	$d_{5/2}$	91	1.48	1.75	$\frac{5}{2}^+$	0.02 [b]	1.0	0.45	5,34
		93	none						
		95	1.74	1.30	$\frac{5}{2}^+$	0.03 [b]	2.0	0.29	present
	$s_{1/2}$	91	2.58	2.96	$\frac{1}{2}^+$	0.24	26	0.54	5
		93	1.94	2.34	$\frac{1}{2}^+$	0.21	3.5	0.08	13
		95	2.28	2.25	$\frac{1}{2}^+$	(0.12)	$\geq$18	$\geq$0.38	present
	$d_{3/2}$	91	3.70	3.81	$\frac{3}{2}^+$	0.10	$\geq$ 8.0	$\geq$0.25	5
		93	3.29	2.83	$\frac{3}{2}^+$	0.03	$\geq$ 8.0	$\geq$0.25	13
		95	2.84	2.93	$\frac{3}{2}^+$	0.10	13.3	0.41	present
2_1^+	$d_{5/2}$	91	(2.06)	2.18	$\frac{3}{2}^+$	0.45	$\geq$ 4.1	$\leq$1.0	5
	$s_{1/2}$	91	3.11	3.39	$\frac{3}{2}^+$	0.11	15	0.31	5
		95	(1.32)	1.85	$(\frac{5}{2}^+)$	0.02	~22	~0.46	present
		95	(2.32)	1.85	$\frac{3}{2}^+$	(0.12)	18	0.37	present
3_1^-	$d_{5/2}$	91	(2.79)	2.75					5
		95	2.02	2.06	$\frac{11}{2}^-$	0.17			53
	$s_{1/2}$	91	(3.83)	3.96					5
		93	3.41	3.29	$\frac{7}{2}^-$		(14.2)	(0.30)	13
		95	3.06	3.01	$\frac{7}{2}^-$		(5.4)	(0.11)	present
		97	(1.82)	1.90					52
	$d_{3/2}$	97	(3.05)	3.01					52

[a] From Ref. 11.

[b] Corrected for $J^\pi = \frac{5}{2}^+$.

els persist as "good" core states in ^{93}Zr and ^{95}Zr. This was to be expected from the trend observed in recent (t,p) [18] and (p,t) [48] reactions on the even Zr isotopes. The energies of the $[0_2^+ \otimes lj]$ parent states are close to the expected zeroth-order positions $E_{clj} = E_c + E_{lj}$ (column five), where E_c denotes the excitation energy of the core state, and E_{lj} the energy of the parent state with the largest (d,p) spectroscopic factor $S_{0lj} \approx 0.5$–1.0 (Ref. 11).[49] The average energy displacement of the actual parent states with respect to E_{clj} is 100–250 keV; it is negative for ^{91}Zr and positive for ^{95}Zr. This change of sign may be accidental, as the spectroscopic factors in the 0_2^+ channel deduced from (p,p') data (see below) differ from those of the respective $[0_1^+ \otimes lj]$ states, but it could also be caused by the relative positions of the 2_1^+ state in ^{90}Zr and ^{94}Zr. Column seven lists the (d,p) spectroscopic factors,[11] and column eight the measured partial widths Γ_{clj} for the decay into the weak-coupling channel clj. Also included in column eight are the partial widths Γ_{0lj} derived from elastic proton scattering at the analogs of the $[0_1^+ \otimes lj]$ states and averaged over the values quoted in the literature (Refs. 5, 10, 13, 30, 34, 43, 44, Ellis and Haeberli,[50] Robson *et al.*,[51] and Jones *et al.*[52]), as well as those obtained in the present study. It is very encouraging that, for the $s_{1/2}$ and $d_{3/2}$ states, the partial widths are equal within 10% for the three isotopes. This enables us to evaluate single-particle widths from the relation

$$\Gamma^{sp}_{0lj} = \Gamma_{0lj}/S_{0lj}$$

and to use these values in the analysis of the (p,p') data.[2] Adopting $\Gamma_{0s_{1/2}} = 39$ keV, $\Gamma_{0d_{3/2}} = 14$ keV, $S_{0s_{1/2}} = 0.84$, and $S_{0d_{3/2}} = 0.43$, we obtain

$$\Gamma^{sp}_{0s_{1/2}} = 44 \text{ keV}, \quad \Gamma^{sp}_{0d_{3/2}} = 33 \text{ keV},$$

with an estimated uncertainty of 15%. As to the $d_{5/2}$ states, one has to correct $\Gamma_{0d_{5/2}}$ with respect to the different resonance energies of the analogs in ^{91}Zr and ^{93,95}Zr. Taking $E_{0d_{5/2}} = 5.21$ MeV in ^{95}Zr as reference point, we find $\Gamma^{sp}_{0d_{5/2}} = 7.4$ keV, with an uncertainty of 15%. We thus end up with a consistent set of single-particle widths Γ^{sp}_{clj} at the weak-coupling energies E_{clj}. In order to evaluate them at a different channel energy E in the range $0 \leq E \leq E_{clj} + 2$ MeV, we remember that the energy dependence of Γ^{sp} is given essentially by the penetrability P_l of the Coulomb barrier

$$\Gamma^{sp}_{clj}(E) = \Gamma^{sp}_{clj}(E_{clj}) P_l(E)/P_l(E_{clj}) .$$

This procedure gives spectroscopic factors S_{clj} in all inelastic channels relative to the elastic channel and consistent for ^{91,93,95}Zr. The spectroscopic factors S_{clj} listed in column nine were calculated in this manner assuming that, at each IAR, the measured decay width $\Gamma_{c'}$ is entirely due to the weak-coupling partial wave lj. With the single exception of the $[0_2^+ \otimes s_{1/2}]$ state in ^{93}Zr ($S = 0.08$), they range between 0.30 and 0.50, and thus indicate a higher fragmentation of the single-neutron strength than in the elastic channel.

Information on weak-coupling states built on other cores is still incomplete. Five states with large $[2_1^+ \otimes lj]$ admixtures ($S_{clj} \approx 0.40$) and four states of the type $[3^- \otimes s_{1/2}]$ were identified.[53] Figure 13 illustrates a comparison of the actual energies, E_{nc}, and spectroscopic factors, S_{clj}, of weak-coupling states of ^{95}Zr with their respective zero-order values, E_{clj} and S_{0lj}. Besides the limitations of (p,p') angular distributions mentioned above, the weak-coupling model itself imposes restrictions to the application of the analog-resonance technique.

(1) The existence of two low-lying 2^+ states c and the four single-neutron orbits $lj = d_{5/2}$, $s_{1/2}$, $d_{3/2}$, and $g_{7/2}$ creates a large number of basis configurations $[c \otimes lj]$ and allows for a high degree of mixing among them.

(2) If the single-neutron strengths were concentrated in only one state for each lj, we would not be able to observe weak-coupling resonances in excited channels, because their entrance widths would be too small. If, on the other hand, the single-neutron strengths are strongly fragmented, the single-particle concept breaks down. A situation suitable for analog-resonance studies will be found when the single-neutron strengths are distributed over a few levels in a range $\Delta E \approx E_c \approx 2$ MeV for each partial wave lj, while the single-particle con-

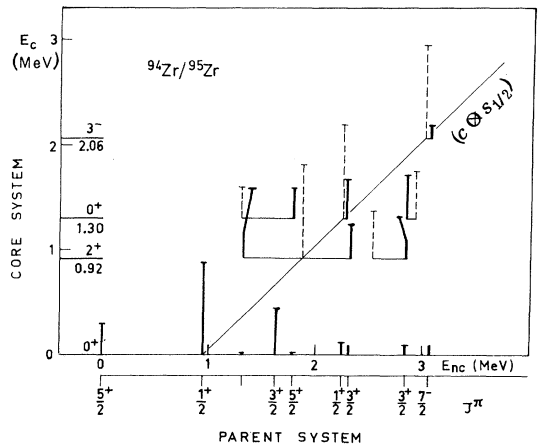

FIG. 13. The measured excitation energies E_{nc} and spectroscopic factors S_{clj} (full lines) of weak-coupling states in ^{95}Zr are compared with their zero-order values $E_{clj} = E_c + E_{lj}$ and S_{0lj} (dashed lines); the abscissa refers to the parent system, the ordinate to the core system.

cept still is meaningful. Due to the fragmentation of the $d_{3/2}$ strength, a number of $[2_1^+ \otimes lj]$ configurations with $J^\pi = \frac{3}{2}^+$ were detected in the Zr region. The even larger distribution of the $f_{7/2}$ strength made the excitation of $[3^- \otimes s_{1/2}]_{7/2}$ configurations possible (but not of $[3^- \otimes d_{5/2}]_{7/2}$ states expected 1 MeV lower).

(3) For a core with $J_c \neq 0$, the range of possible spin values $\vec{J} = \vec{J}_c + \vec{j}$ is quite large, in general. However, only a small number can be reached in the elastic channel. Considering the concentration of the $d_{5/2}$ strength in the Zr isotopes, and the very small single-particle widths for $g_{7/2}$ and $h_{11/2}$ waves, we expect only resonances with $J^\pi = \frac{1}{2}^+$, $\frac{3}{2}^+$, and $\frac{7}{2}^-$, as realized in the experiment. We also point out that none of the $\frac{3}{2}^-$ assignments made in the (d,p) work[11] could be established in analog-resonance studies.

5. CONCLUSIONS

Differential cross sections for elastic and inelastic proton scattering on ^{94}Zr were measured over the analog resonances of states in ^{95}Zr between 0.95- and 3.10-MeV excitation energy. In order to line up the parent and analog spectra, the reactions ^{94}Zr(d,p) and ^{94}Zr$(d,p\gamma)$ were also studied using a magnetic spectrometer and a Ge(Li) detector (Table I).

The data were analyzed in the framework of Weidenmüller's theory, with the particular aim to identify the angular momenta of protons in the inelastic channels and to deduce partial widths and spectroscopic factors. To this end, contributions in the cross section arising from nonresonant processes, such as Hauser-Feshbach contributions and direct excitation, had to be taken into account. The enhancement of the Hauser-Feshbach background due to isospin mixing was found to be negligible for strong resonances above the (p,n) threshold. Inclusion of a DWBA cross section improved the fits to the shapes and the magnitudes of off-resonance angular distributions in the 0.92-MeV (2^+) and 2.06-MeV (3^-) channels. Interference of this DWBA amplitude with the resonant amplitude was found also to explain the observed asymmetric resonance shapes and deviations in the angular distributions from symmetry about 90°. The optical proton potential between 6.0- and 8.5-MeV bombarding energy agrees well with that determined at 12.7 MeV, and with the optical potential of the $|nc\rangle$ system adjusted to fit the binding energies of the $s_{1/2}$ and $d_{3/2}$ single-neutron parent states in ^{95}Zr.

Even after careful correction for Hauser-Feshbach and DWBA contributions many on-resonance angular distributions could not be analyzed because of ambiguities caused by the mixture of several partial waves in excited channels. In the present case, this problem seems by far more serious than the interference with direct excitation. Polarized beam and $(p,p'\gamma)$ correlation experiments would appear very promising for eliminating these ambiguities. These measurements would test the results of the present study for IAR where the partial wave of the outgoing protons was identified (for instance, at 7.58, 6.54, 7.91, 8.11, and 8.26 MeV) and would help to determine the components not resolved in our work. At 7.6-MeV proton energy a double resonance was found, both states probably having $J^\pi = \frac{3}{2}^+$; more data are required in order to make a two-level analysis meaningful. An attempt to calculate single-particle widths in the elastic channel adopting the methods of Zaidi and Darmodjo[21] and of Thompson[22] was unsuccessful: discrepancies in the spectroscopic factors between the (d,p) and (p,p_0) range up to 40% in both directions. To derive single-particle widths from the elastic channel $\Gamma_{0lj}^{sp} = \Gamma_{0lj}/S_0$, and infer them to inelastic channels turned out to be more appropriate and consistent in all Zr isotopes.

In spite of these obstacles, a considerable amount of spectroscopic information was derived on spins and parities (Table IV) and configurations (Tables II, III, and V) of low-lying states in ^{95}Zr. An upper limit of 5% was set on the $[\nu(d_{5/2})^{-1}\nu(s_{1/2})]_2$ admixture in the wave function of the lowest 2^+ state in ^{94}Zr. As in ^{90}Zr, the 0_2^+ and 3_1^- levels in ^{94}Zr proved to be "good" core states in the sense of the weak-coupling model, better even than in ^{92}Zr (Table V). As to the 2^+ core states, some of the $[2_1 \otimes s_{1/2}]$ and $[2_1 \otimes d_{3/2}]$ strength is concentrated $(S_{cl'j'} \approx 0.40)$ in $J^\pi = \frac{3}{2}^+$ states. However, the existence of two low-lying 2^+ states in ^{94}Zr and ^{92}Zr, the large number of basis configurations which mix with each other, and the difficulties in resolving these mixtures make inelastic proton scattering an insufficient tool to draw any conclusion on this point. It is also worthwhile to note that most analogs show up in the excitation functions to the lowest 2^+ state in ^{90,92,94}Zr, in spite of the different shell-model wave functions of these states, and that all higher states are populated more selectively.

ACKNOWLEDGMENTS

It is a pleasure to acknowledge illuminating conversations with Dr. T. Tamura and his continuous help in handling the programs NEPTUNE and JUPITER. We are indebted to Dr. W. J. Thompson and Dr. C. F. Moore for valuable comments on the weak-coupling model, and to J. Kulleck and T. Ragland for assistance in data taking. The assistance

of C. Hollas and H. R. Hiddleston in using computer programs for the interactive display function of the CDC 6600 computer is appreciated. One of us (K.P.L.) appreciated the financial aid of a Fulbright Fellowship at The University of Texas during 1968–1969.

---

†Work supported in part by the U. S. Atomic Energy Commission, the Robert Welch Foundation, and the German Bundesministerium für Wirtschaftliche Zusammenarbeit.

*Present address: Van de Graaff Accelerator Laboratory, Ohio State University, Columbus, Ohio 43212.

‡Present address: Reaktorzentrum der Oesterreichischen Studiengesellschaft für Atomenergie, Seibersdorf, NO, Austria.

[1]G. A. Jones, A. M. Lane, and G. C. Morrison, Phys. Letters 11, 329 (1964).

[2]J. P. Bondorf, P. von Brentano, and P. Richard, Phys. Letters 27B, 5 (1968).

[3]N. Auerbach, Phys. Letters 27B, 127 (1968).

[4]C. F. Moore, J. J. Kent, and S. A. A. Zaidi, Phys. Rev. Letters 18, 345 (1967).

[5]K. P. Lieb, T. Hausmann, J. J. Kent, and C. F. Moore, Phys. Rev. 175, 1482 (1968).

[6]K. P. Lieb, T. Hausmann, and J. J. Kent, Phys. Rev. 182, 1341 (1969).

[7]K. P. Lieb, T. Hausmann, J. J. Kent, and C. F. Moore, Z. Physik 217, 213 (1968).

[8]J. K. Dickens, E. Eichler, and G. R. Satchler, Phys. Rev. 168, 1355 (1968).

[9]T. Hausmann and K. P. Lieb, Phys. Rev. Letters 23, 137 (1969).

[10]K. Wienhard, G. Clausnitzer, G. Graw, and R. Fleischmann, Z. Physik 228, 129 (1969).

[11]B. L. Cohen and O. V. Chubinsky, Phys. Rev. 131, 2184 (1963).

[12]M. M. Stautberg, R. R. Johnson, J. J. Kraushaar, and B. W. Ridley, Nucl. Phys. A104, 67 (1967).

[13]J. J. Kent, K. P. Lieb, and C. F. Moore, Phys. Rev. C 1, 336 (1970).

[14]A. E. S. Green, R. J. Berkley, C. E. Watson, and C. F. Moore, Rev. Sci. Instr. 37, 415 (1966); J. Amezquita, C. F. Moore, K. P. Lieb, J. G. Kulleck, M. Koike, and C. E. Watson, Nucl. Phys. A146, 26 (1970).

[15]D. Robson, Phys. Rev. 137, B535 (1965); A. K. Kerman, in *Proceedings of the Second Conference on Nuclear Isospin, Asilomar-Pacific Grove, California, 13–15 March 1969*, edited by J. D. Anderson, S. D. Bloom, J. Cerny, and W. W. True (Academic Press Inc., New York, 1969).

[16]P. von Brentano, in Proceedings of the Symposium on Nuclear Physics, Tiblisi, U.S.S.R., 1967 (to be published).

[17]E. C. Bartels, E. R. Cosman, A. K. Kerman, and J. A. Spencer, Phys. Rev. 179, 995 (1969).

[18]J. G. Beery, Los Alamos Scientific Laboratories Report No. LA-3958, 1968 (unpublished).

[19]J. Vervier, Nucl. Phys. 75, 17 (1965).

[20]H. A. Weidenmüller, Nucl. Phys. A99, 269 (1969); C. Mahaux and H. A. Weidenmüller, *Shell-Model Approach to Nuclear Reactions* (John Wiley & Sons, New York, 1969), Chap. 13.

[21]S. A. A. Zaidi and S. Darmodjo, Phys. Rev. Letters 19, 1446 (1967); S. Darmodjo, Ph.D. thesis, University of Texas, 1968 (unpublished); P. A. Moore, Ph.D. thesis, University of Texas, 1969 (unpublished).

[22]W. J. Thompson, Nucl. Data A6, 129 (1969).

[23]A. M. Lane, Nucl. Phys. 35, 676 (1962).

[24]R. O. Stephen, Nucl. Phys. A94, 192 (1967).

[25]T. Tamura, computer code NEPTUNE, 1968, private communication.

[26]G. R. Satchler, R. M. Drisko, and R. H. Bassel, Phys. Rev. 136, B637 (1964).

[27]H. L. Harney, Nucl. Phys. A119, 591 (1968).

[28]G. W. Bund, Ph.D. thesis, University of Washington, 1968 (unpublished).

[29]H. L. Harney and H. A. Weidenmüller, Nucl. Phys. A139, 241 (1969); H. L. Harney, C. A. Wiedner, and J. P. Wurm, Phys. Letters 26B, 204 (1968).

[30]W. J. Thompson and J. L. Ellis, in *Proceedings of the Second Conference on Nuclear Isospin, Asilomar-Pacific Grove, California, 13–15 March 1969*, edited by J. D. Anderson, S. D. Bloom, J. Cerny, and W. W. True (Academic Press Inc., New York, 1969); W. J. Thompson, J. Adams, and D. Robson, Phys. Rev. 173, 975 (1968).

[31]E. Abramson, I. Plesser, Z. Vager, and J. P. Wurm, Phys. Letters 29B, 304 (1969).

[32]K. P. Lieb, to be published; K. P. Lieb, J. J. Kent, T. Hausmann, and C. E. Watson, Phys. Letters 32B, 273 (1970).

[33]E. Sheldon and D. M. Van Patter, Rev. Mod. Phys. 38, 43 (1966).

[34]H. L. Scott, C. P. Swann, and F. Rauch, Nucl. Phys. A134, 667 (1969); K. P. Lieb and D. Burch, Z. Physik 234, 161 (1970).

[35]U. Gruber *et al.*, Nucl. Phys. 67, 433 (1965); E. T. Jurney *et al.*, Nucl. Phys. A111, 105 (1968); J. B. Moorhead, and R. A. Moyer, Phys. Rev. 184, 1205 (1969).

[36]J. M. Beyster, Los Alamos Scientific Laboratory Report No. LA-2099, 1956 (unpublished).

[37]T. Tamura, Rev. Mod. Phys. 37, 679 (1965); T. Tamura, J. Phys. Soc. Japan Suppl. 24, 288 (1968).

[38]M. M. Stautberg and J. J. Kraushaar, Phys. Rev. 151, 969 (1966).

[39]H. J. Kim, J. K. Bair, C. M. Jones, and H. B. Willard, Phys. Rev. 186, 1110 (1969).

[40]About 25% of the cross section in the 2^+ channel at 6.29 MeV, $\sigma = 2.2$ mb, may be attributed to direct excitation as predicted by JUPITER.

[41]T. Tamura, Oak Ridge National Laboratory Report No. ORNL-4152, 1967 (unpublished).

[42]S. Devons and L. J. B. Goldfarb, in *Encyclopedia of Physics*, edited by S. Flugge (Springer-Verlag, Berlin, Germany, 1957), Vol. 42, p. 362.

[43]J. C. Legg, M. A. Crosby, and G. Roy, Phys. Letters 20, 399 (1966).

[44]J. D. Fox, private communication, quoted in N. Cue and P. Richard, Phys. Rev. 173, 1108 (1968).

[45]L. N. Galperin, A. Z. Ilyasov, I. K. Lemberg, and G. A. Firsanov, Yadern, Fiz. 9, 225 (1969) [transl.: Soviet J. Nucl. Phys. 9, 133 (1969)].

[46]S. Cochavi, N. Cue, and D. B. Fossan, Phys. Rev. C 1, 1821 (1970). These authors interpret the longer lifetimes of the 0_2^+ and 2_1^+ states in ^{94}Zr as a consequence of stronger mixing of the proton configurations in ^{94}Zr than in ^{92}Zr. This is not conclusive, however, as a stronger mixing of the neutron configurations would produce the same effect.

[47]H. L. Harney, Phys. Letters 28B, 249 (1968).

[48]J. B. Ball, R. L. Auble, and P. G. Roos, Phys. Letters 29B, 172 (1969).

[49]It would be more consistent to consider the respective "centers of gravity" $\bar{E}_{lj}$ instead of just the predominant component E_{lj} of the single-particle strengths. However, this would require more information of the fragmentation of the strengths than is available at the present time.

[50]J. L. Ellis and W. Haeberli, in *Proceedings of the Second Conference on Nuclear Isospin, Asilomar–Pacific Grove, California, 13–15 March 1969,* edited by J. D. Anderson, S. D. Bloom, J. Cerny, and W. W. True (Academic Press Inc, New York, 1969).

[51]D. Robson, J. D. Fox, P. Richard, and C. F. Moore, Phys. Letters 18, 86 (1965).

[52]R. R. Jones, P. Dyer, C. F. Moore, G. Morrison, and N. Williams, Bull. Am. Phys. Soc. 13, 562 (1968).

[53]W. Booth, S. M. Dalgliesh, K. C. McLean, R. N. Glover, and F. R. Hudson, Phys. Letters 30B, 335 (1969).

PHYSICAL REVIEW C VOLUME 2, NUMBER 5 NOVEMBER 1970

Production and Decay Properties of Protactinium Isotopes of Mass 222 to 225 Formed in Heavy-Ion Reactions*

Jørn Borggreen,† Kalevi Valli,‡ and Earl K. Hyde
Nuclear Chemistry Division, Lawrence Radiation Laboratory, University of California, Berkeley, California 94720

(Received 11 May 1970)

Four α-decay chains initiated by ^{225}Pa, ^{224}Pa, ^{223}Pa, and ^{222}Pa were produced by the bombardment of thallium, lead, and bismuth targets with beams of ^{22}Ne, ^{20}Ne, ^{19}F, ^{18}O, ^{16}O, ^{15}N, and ^{14}N at the Berkeley heavy-ion linear accelerator. The reaction products were transported from the reaction cell by the helium-jet technique and their decay was measured with a semiconductor detector. Energy values, excitation functions, half-lives, and genetic relationships of individual peaks were determined. Two new techniques based on the use of a time-to-amplitude converter were developed for the measurement of μsec half-lives of daughter products, and five half-lives in the μsec range were measured.

These new α data help to determine the trends in α-decay energies for isotopes of odd-Z elements, particularly in the poorly defined region just above the 126-neutron shell. This allows more accurate predictions of α-decay properties of many unknown nuclei. Some anomalous behavior of the apparent α-decay energies for nuclei with 133 and 135 neutrons is pointed out.

I. INTRODUCTION

In a recent paper[1] we have presented new information on thorium isotopes of mass 221 to 224 and on the radium and radon isotopes into which they decay. These nuclides fall in that part of the nuclide chart just above the 82-proton and 126-neutron shells where nuclear information has been sparse because of the instability of the nuclei and the difficulty of making them. Reactions induced by complex nuclear projectiles such as ^{14}N, ^{16}O, ^{19}F, ^{20}Ne, and ^{22}Ne in such targets as thallium, lead, and bismuth provide one means of reaching this region of the nuclide chart. The previous paper was restricted to a study of nuclides of even atomic number prepared by such reactions. In the present paper we discuss results on odd-Z products, specifically the α-decay chains initiated by ^{225}Pa, ^{224}Pa, ^{223}Pa, and ^{222}Pa. Figure 1 shows the four series about which new information was obtained in this study and shows their location in the chart of the nuclides.

This study was conducted because of the intrinsic interest in the decay properties of unknown nuclei, particularly those far from β stability. Such α-decay data are also useful for making estimates of ground-state masses, for testing the predictions of atomic-mass equations and prescriptions, and for other matters related to the systematic trends in ground-state properties.

An additional reason for this study is the need for background information for a proper interpretation of α-particle data obtained in nuclear reactions involving transuranium element targets. There is an intense interest in reactions which provide information on nuclides of charge greater